



Differential vulnerability of the cerebellum in healthy ageing and Alzheimer's disease

Helena M. Gellersen, Xavier Guell, Saber Sami

PII: S2213-1582(21)00049-8
DOI: <https://doi.org/10.1016/j.nicl.2021.102605>
Reference: YNICKL 102605



Available online at www.sciencedirect.com
ScienceDirect

To appear in: *NeuroImage: Clinical*

Received Date: 27 October 2020
Revised Date: 12 January 2021
Accepted Date: 15 February 2021

Please cite this article as: H.M. Gellersen, X. Guell, S. Sami, Differential vulnerability of the cerebellum in healthy ageing and Alzheimer's disease, *NeuroImage: Clinical* (2021), doi: <https://doi.org/10.1016/j.nicl.2021.102605>

This is a PDF file of an article that has undergone enhancements after acceptance, such as the addition of a cover page and metadata, and formatting for readability, but it is not yet the definitive version of record. This version will undergo additional copyediting, typesetting and review before it is published in its final form, but we are providing this version to give early visibility of the article. Please note that, during the production process, errors may be discovered which could affect the content, and all legal disclaimers that apply to the journal pertain.

Differential vulnerability of the cerebellum in healthy ageing and Alzheimer's disease

Helena M. Gellersen^{1*}, Xavier Guell², Saber Sami³

¹Behavioural and Clinical Neuroscience Institute (BCNI), Department of Psychology, University of Cambridge, Cambridge, UK; hg424@cam.ac.uk

²Massachusetts Institute of Technology, Massachusetts General Hospital, and Harvard Medical School, USA; xaviergp@mit.edu

³Norwich Medical School, Faculty of Medicine and Health Sciences, University of East Anglia, Norwich Research Park, Norwich, UK; s.sami@uea.ac.uk

*Corresponding author

Addresses:

¹BCNI
Sir William Hardy Building
Downing Street
Cambridge CB2 3EB
United Kingdom

²Massachusetts Institute of Technology
77 Massachusetts Avenue
Cambridge, MA
USA

³Norwich Medical School
Norwich Research Park
Norwich NR4 7TJ
United Kingdom

Declaration of interest: None.

Author note: H.M.G. is supported by a grant from the Medical Research Council [award number RG86932]. The funder had no role in study design, analysis, writing or the decision to submit the article for publication.

Abstract

Recent findings challenge the prior notion that the cerebellum remains unaffected by Alzheimer's disease (AD). Yet, it is unclear whether AD exacerbates age-related cerebellar grey matter decline or engages distinct structural and functional territories. We performed a meta-analysis of cerebellar grey matter loss in normal ageing and AD. We mapped voxels with structural decline onto established brain networks, functional parcellations, and along gradients that govern the functional organisation of the cerebellum. Importantly, these gradients track continuous changes in cerebellar specialisation providing a more nuanced measure of the functional profile of regions vulnerable to ageing and AD. Gradient 1 progresses from motor to cognitive territories; Gradient 2 isolates attentional processing; Gradient 3 captures lateralisation differences in cognitive functions. We identified bilateral and right-lateralised posterior cerebellar atrophy in ageing and AD, respectively. Age- and AD-related structural decline only showed partial spatial overlap in right lobule VI/Crus I. Despite the seemingly distinct patterns of AD- and age-related atrophy, the functional profiles of these regions were similar. Both participate in the same macroscale networks (default mode, frontoparietal, attention), support executive functions and language processing, and did not exhibit a difference in relative positions along Gradients 1 or 2. However, Gradient 3 values were significantly different in ageing vs. AD, suggesting that the roles of left and right atrophied cerebellar regions exhibit subtle functional differences despite their membership in similar macroscale networks. These findings provide an unprecedented characterisation of structural and functional differences and similarities in cerebellar grey matter loss between normal ageing and AD.

Keywords: cerebellum, aging, Alzheimer's disease, grey matter loss, functional gradients

1. Background

Despite the earlier notion that the cerebellum is spared in Alzheimer's disease (AD), recent studies have started to elucidate detrimental effects of AD on cerebellar structure, which in some cases correlates with clinical disease ratings (Gellersen et al., 2017; Guo et al., 2016a; Jacobs et al., 2018; Serra et al., 2017; Toniolo et al., 2018). This is in line with the current understanding that the cerebellum is involved in a range of cognitive, motor, and affective functions by virtue of segregated cerebro-cerebellar loops (Kelly & Strick, 2003; Schmahmann, Guell, Stoodley, & Halko, 2019). Cerebellar grey matter loss does not only occur in AD, but the healthy ageing process is also associated with changes in cerebellar structure, which are comparable in magnitude to those observed in the prefrontal cortex and hippocampus (Bernard & Seidler, 2014; Jernigan et al., 2001; Raz & Rodrigue, 2006). These marked alterations highlight the importance of the cerebellum for our understanding of both cognitive ageing and Alzheimer's disease processes.

However, it is unclear if these AD-related changes exacerbate existing negative effects of ageing on the cerebellum or whether they additionally target regions less vulnerable to normal ageing processes. Moreover, a direct comparison of the functional characterisation of regions affected by ageing and AD is also still lacking. Here we combine a coordinate-based meta-analytic approach to identify the most consistent patterns of grey matter loss across studies with multiple complimentary functional mappings to advance our understanding of cerebellar vulnerability to normal ageing and Alzheimer's disease (Buckner, Krienen,

Castellanos, Diaz, & Yeo, 2011; Eickhoff, Bzdok, Laird, Kurth, & Fox, 2012; Guell et al., 2019; Guell, Schmahmann, Gabrieli, & Ghosh, 2018; King, Hernandez-Castillo, Poldrack, Ivry, & Diedrichsen, 2019).

The importance of the cerebellum for multiple cognitive, affective and motor domains is increasingly being recognised (Schmahmann et al., 2019), as is its role in age- and AD-related functional changes (Bernard et al., 2020; Bernard & Seidler, 2014; Gellersen et al., 2017; Jacobs et al., 2018). Despite the striking uniformity of cerebellar cellular organisation, the anterior-posterior functional continuum from motor to cognitive regions and the unique cortico-limbic connectivity patterns of each cerebellar lobule suggest non-uniformity of age and pathological effects across this brain region (Bernard, Leopold, Calhoun, & Mittal, 2015; Buckner et al., 2011; Koppelmans et al., 2017; Ramanoël et al., 2018). Indeed, effects of AD are not uniform across cerebellar lobules. In a previous meta-analysis, consistent patterns of AD-related cerebellar atrophy across studies were found in posterior cerebellar lobules (Gellersen et al., 2017), although since then other authors demonstrated that grey matter loss may also occur in anterior lobules of the cerebellum in AD and depends on disease progression (Toniolo et al., 2018).

An important question concerns the interpretation of these structural findings with respect to potential consequences for function. There are now multiple maps of cerebellar functional organisation derived from task-based fMRI to identify discrete functional boundaries (King et al., 2019), or based on resting-state intrinsic connectivity which define different brain networks (Buckner et al., 2011) or explain connectivity patterns in terms of a region's relative position along major cerebellar functional gradients, respectively (Guell et al., 2018). Three major gradients have been shown to govern the functional architecture of the cerebellum: the first tracks the

transition between cognitive to motor regions, the second defines the extent to which a region is engaged in a task-positive processing thereby isolating attentional components, and the third captures laterality asymmetries in the left compared to the right cerebellar hemisphere that are specific to non-motor processes. As such, the third gradient suggests that cognitive processing in left and right hemispheres may be qualitatively different, a notion that may not be visible when only using the established network-specific mappings of the cerebellum (Buckner et al., 2011). The unique feature of the gradient-based approach is that each cerebellar voxel is characterised based on its position along the continuum between the two extremes of each functional gradient. As a result, voxels do not have to be categorised into one of the functional networks or parcels (as is the case in Buckner et al., 2011; King et al., 2019), but can take on any position along the functional spectrum allowing for a comparison of the relative functional preferences of regions vulnerable to AD and normal ageing.

All of these approaches provide complimentary information about cerebellar functional organisation: the network-based approach puts cerebellar regions into context with the functional characterisation of the neocortex (Buckner et al., 2011); the discrete parcellation allows for a direct mapping of specific cognitive, motor and affective processes onto cerebellar anatomical subregions (King et al., 2019); and the gradient-based approach presents a picture of gradual changes in functional preferences across major functional axes, refraining from defining discrete boundaries and allowing each region to be characterised by multiple features (Guell et al., 2018). These gradients also provide information regarding the relationship between different functional territories of the cerebellar cortex, an important piece of information which is absent in discrete maps of cerebellar functional neuroanatomy. The use of all three

methods for the interpretation of functional consequences of grey matter atrophy is therefore synergistic.

Yet, in most studies, the interpretation of implications of age- or AD-dependent structural decline for cerebellar function is based on the location of the identified cluster within a given lobule (Bernard et al., 2015; Bernard & Seidler, 2013; Buhrmann et al., 2020). While valuable, such an approach may miss further subtler functional differences within a region or continuities between regions that only become apparent on non-discrete mappings. Moreover, functional territories do not neatly map onto macroscale anatomical boundaries (King et al., 2019).

Here, we used the discrete and network-based maps in combination with the gradient-based approach which allowed us to place our meta-analytic structural imaging findings on multiple functional maps and to compare those derived from ageing with those from AD. The use of gradients can highlight even subtle functional differences between neuroanatomical regions vulnerable to AD and normal ageing (Guell et al., 2018), which can be put into context with discrete mappings that have typically been used by most prior studies. These investigations will further our understanding of the role that grey matter decline in the cerebellum may play in functional deficits and will demonstrate whether these patterns of age-related grey matter loss are distinct from those in Alzheimer's disease.

2. Methods

2.1 Literature Search

We carried out a systematic literature search on Pubmed and PsycInfo using search terms related to ageing and structural neuroimaging in the title and/or abstracts of peer-reviewed records that were published until October 1st 2019. Inclusion criteria

required 1) an analysis that compared grey matter volume in healthy young (< 40 years) and older participants (60+ years), and 2) availability of coordinates of regions with grey matter decline (either from a whole-brain analysis or from a region of interest analysis that included the cerebellum). Studies were excluded if 1) participants had psychiatric or neurological conditions, 2) the cerebellum was excluded from the analysis, 3) the study used confounding factors besides covariates sex, age and education in the analysis, and 4) the study reanalysed previously published data already included in our meta-analysis. We extracted sample size, participant demographics, coordinates of cerebellar grey matter loss and information regarding the statistical analysis from each included study. All coordinates reported in Talairach space were converted to MNI space using the `icbm2tal` transform employed by the conversion tool provided by GingerALE (brainmap.org).

$N=18$ studies were identified for inclusion in the meta-analysis. Input for the analysis were coordinates of age-related decreased cerebellar grey matter volume or density and the sample size of each study. We also conducted an updated analysis of cerebellar grey matter decline in late-onset AD in $n=13$ studies based on our previous research (Gellersen et al., 2017) and studies published since then (Ahmed et al., 2019; Toniolo et al., 2018). The details of the literature search for the AD meta-analysis are shown in Gellersen et al. (2017). Studies with early-onset AD and atypical forms of AD were excluded from the meta-analysis to reduce heterogeneity in patient samples. Most patients had mild to moderate AD (Table B2).

For details on search terms and the PRISMA flowchart for study selection see Appendix A. For a list of participants, imaging parameters, cerebellar coordinates, cognitive deficits (age- and AD-related) and associations between cerebellar grey

matter and cognitive performance see Appendix B (Table B1 for healthy ageing and Table B2 for AD).

2.2 Meta-Analysis

The coordinate-based random-effects meta-analyses on age and AD were carried out using anatomical likelihood estimation (ALE) using version 2.3.6 of GingerALE (<http://brainmap.org>) (Eickhoff et al., 2012, 2009; Turkeltaub, Eden, Jones, & Zeffiro, 2002). In the coordinate-based meta-analysis, every coordinate, referred to as a “focus”, is treated as the centre of a Gaussian probability distribution with a full-width half-maximum based on the sample size of the respective experiment. For each study, a modelled activation (MA) map of grey matter differences between age groups was formed by finding the maximum across the Gaussian probability distributions of all foci. The final ALE image that represents the results of the meta-analysis is created from the union of the MA maps of all studies. To determine the null distribution of the ALE statistic, values from the MA maps are sorted to create histograms. Histograms are then divided by the number of voxels in a map to generate probabilities for each value of the MA map. Based on these, p -value images are created which can then be used for thresholding.

For the current analysis, a cluster-level thresholding method was chosen. This method simulates random data sets with the same characteristics of the original data set used to create the ALE image, namely the total number of foci, number of foci groups, and sample sizes. A probability threshold is then set by selecting a minimum number of voxels per cluster in a way that only a certain amount of the clusters in the simulated data sets exceed this minimum size. In the case of this analysis, we chose a $p < .05$ for cluster-level family-wise error correction (i.e. the cluster-level inference option on GingerALE), which provides the best compromise between sensitivity and specificity

(Eickhoff et al., 2016). The cluster-forming threshold was chosen to be $p < .001$ (uncorrected), which is one of the two thresholds recommended by GingerALE (Laird et al., 2005). To demonstrate the convergence between these analyses, we created a conjunction image in GingerALE based on the voxelwise minimum between the two thresholded ALE images derived from the AD and the ageing analyses (Eickhoff et al., 2012, 2011).

It is important to note that a region of interest (ROI) based meta-analysis does not provide information about the likelihood or prevalence of cerebellar atrophy in older adults and AD but rather characterises the pattern of lobular grey matter loss in cases where cerebellar atrophy is indeed present.

2.3 Visualisation of meta-analytic results

We used the SUI toolbox to create multiple cerebellar maps, which are created by unfolding and flattening the cerebellar surface to obtain a 2D representation (Diedrichsen, Balsters, Flavell, Cussans, & Ramnani, 2009; Diedrichsen et al., 2011; Diedrichsen & Zotow, 2015). Note that the flatmap is not a true surface reconstruction and is based on volumetric MRI data (Diedrichsen & Zotow, 2015).

To put our structural findings into context, we used three maps of the functional organisation of the cerebellum that have been derived on the basis of cerebellar functional activation and cortico-cerebellar connectivity patterns: 1) the Buckner networks based on intrinsic connectivity derived from resting-state fMRI showing the membership of different cerebellar subregions to one of the established functional connectivity networks of the brain (Buckner et al., 2011), 2) the King et al. (2019) map based on a multi-domain cognitive task battery, and 3) a gradient-based, continuous map of the functional preferences of different cerebellar regions (Guell et

al., 2018), which can be used to quantify relative differences in the functional characteristics of cerebellar voxels (see section 2.4).

2.4 Using gradients to quantify relative differences in functional preferences of regions with grey matter loss in ageing and Alzheimer's disease

To further add to the topographical interpretation of our meta-analytic findings, we used a recently developed tool called LittleBrain (Guell et al., 2019; <https://xaviergp.github.io/littlebrain/>). LittleBrain maps the voxels identified in our structural analysis onto gradients that capture low-dimensional properties of cerebellar functional organization that has previously been described using a non-linear dimensionality reduction method called diffusion map embedding on Human Connectome Project functional resting-state data (Guell et al., 2018; Margulies et al., 2016). The method identified the functional relationships of intrinsically connected cerebellar voxels, which may not be directly connected through cerebellar neocortical association fibres but likely participate in similar functional cerebro-cerebellar loops. Diffusion map embedding defined components that account for as much of the variability in the data as possible, similar to linear methods such as principal component analysis, with the crucial distinction that voxels were not assigned to separate networks. This mapping method therefore overcomes the limitation of being constrained by discrete boundaries established through structural parcellation and can identify the progressive hierarchical functional organisation across cerebellar regions as has previously been achieved for the neocortex (Margulies et al., 2016). The method allowed for overlap between functional gradients such that each voxel has a position in each gradient (Guell et al., 2018). Note that voxels that are close in the gradient dimensions exhibit similar functional connectivity patterns.

The gradient-based map demonstrated that the functional macroscale organisation of the cerebellum can be characterised as following along two principal gradients. Cerebellar Gradient 1 represents the principal functional axis of the cerebellum, including motor representations on one extreme (lobules IV-VI and VIII) and transmodal cognitive processing such as cerebellar default mode network regions on the other (Crus I/II and lobule IX). Gradient 2 isolates attentional processes moving along a task-focused to task-unfocused functional axis (Guell et al., 2018). One end of this gradient includes anterior regions Crus I/II involved in the frontoparietal and attention networks, while the other end includes motor (lobules I-IV) and DMN regions (posterior Crus I/II). We also chose to include Gradient 3, which captures more subtle aspects of the functional profile of cerebellar regions. Specifically, it demonstrates differences in lateralisation of non-motor functions. This is relevant given that our findings for AD and ageing exhibit differences in hemispheric lateralisation.

After identifying regions of grey matter loss, we created plots of the position that each of the voxels with grey matter loss in aging, AD and the Aging-AD conjunction held along the three functional gradients. Furthermore, each voxel was colour-coded according to its participation in the cerebro-cerebellar resting-state networks identified in Buckner et al. (2011).

Gradient values were extracted for further statistical analyses to determine whether the distribution along each gradient for the aging and AD effects differed from one another. Due to non-normality of the true gradient value distributions (Shapiro-Wilk tests: $W > .8$, $p < .001$), differences between the AD and ageing gradient values were tested using permutation testing of differences in rank sums. Gradient values were assigned to the AD and ageing group randomly and the rank sums

between the real observed and random differences between the two groups were tallied. The reported p -value for the permutation test represents the probability of getting the observed differences in gradient values between the true AD- and true age-related voxels from random group assignments of each voxel in the permutation procedure.

We also computed the non-parametric effect sizes Cohen's U_I (Cohen, 1988) using the Matlab toolbox "Measures of Effect Size" (Hentschke & Stüttgen, 2011): Cohen's U_I can be interpreted as the proportion of scores across both groups within the areas of no overlap, such that completely separate distributions result in $U_I=1$ (large effect) and completely overlapping distributions have $U_I=0$ (null effect) (Cohen, 1988; Hentschke & Stüttgen, 2011).

The distributions of gradient values were visualised using violin plots in ggplot2 in RStudio version 1.0.153 (Wickham, 2016).

2.5 Robustness tests: jackknife procedure

The robustness of our results for the ageing and AD analyses, respectively, to the removal of studies was tested using a jackknife procedure, in which the meta-analysis was carried out without a given study. As a result, 18 one-study removed analyses were carried out for the ageing dataset and 13 such analyses were carried out for the AD dataset, in which we conducted the ALE meta-analysis without a given study. We also tested whether the difference in the distribution of AD gradient values and the jackknife analysis gradient values remained robust to the removal of any one study. Our results regarding age- and AD-related atrophy regions and differences in gradient values between ageing and AD remained robust across jackknife analyses (for details see Appendix D).

3. Results

3.1 Healthy ageing meta-analysis

The ageing analysis involved 18 studies with 64 coordinates of cerebellar grey matter atrophy across 2441 subjects (Appendix B, Table B1 for details of included studies). Five clusters of reduced grey matter volume were identified (Fig. 1a, Table 1; all local peaks $p < .020$). Cluster 1 was situated in right Crus II. Cluster 2 encompassed parts of right Crus I and lobule VI. Cluster 3 was in left Crus II. The fourth cluster of grey matter volume reduction was in vermal lobule VI, encroaching upon left hemispheric lobule VI. The fifth cluster was located in lateral left posterior hemisphere with peaks in Crus II and Crus I, with some extension into lobules VIIb and VIII.

3.2 Alzheimer's disease meta-analysis

The final dataset for the AD analysis comprised $n=13$ studies in 529 patients and controls with $k=35$ foci of cerebellar grey matter loss relative to controls. Study characteristics for the included studies can be found in Appendix B (Table B2). The meta-analysis revealed two adjacent AD-related cluster of grey matter loss in the right posterior hemisphere (Fig. 1b; Table 1; all $p < .020$). Cluster 1 included regions of right Crus I and II. Cluster 2 comprised regions of lobule VI and Crus I. The inclusion of the additional studies in this analysis compared to our previous results increased the extent but did not have a substantial effect on the location of the peak coordinates (Gellersen et al., 2017).

3.3 Conjunction between ageing and Alzheimer's disease

The conjunction image generated by GingerALE to compare the AD and ageing results demonstrated that there was one larger region of overlap between these

two groups ($p=.013$; Fig. 1c; Table 1; see also two minor regions of overlap). This was a cluster in right Crus I/lobule VI that had emerged in both analyses.

Table 1. Results of the anatomical likelihood estimation meta-analyses for healthy ageing ($n=18$ experiments with a total of 2441 subjects and $k=64$ foci of cerebellar grey matter decline), Alzheimer's disease ($n=13$ experiments with a total of 529 subjects and $k=35$ foci of cerebellar decline), and the conjunction which identified the spatial overlap between effects of Alzheimer's disease and age on cerebellar structure. Here we report the Montreal Neurological Institute coordinates returned by GingerALE. Labels are according to the spatially unbiased atlas template of the cerebellum and brainstem (SUIT).

Cluster number	Peak MNI coordinates	Extent	Cluster size (mm ³)	p-value	Local extrema	Peak Label	Notes
<i>Healthy ageing</i>							
1	33 -81 -37	24 -90 -42 to 40 -72 -30	1504	.018 .015	36 -80 -38 30 -88 -34	R Crus II	
2	35 -63 -29	28 -70 -34 to 42 -56 -22	1464	.018	36 -60 -30	R Crus I	Extends into VI
3	-35 -77 -40	-46 -86 -44 to -28 -68 -34	1288	.018 .016 .011	-34 -82 -38 -34 -72 -40 -42 -76 -40	L Crus II	
4	1 -72 -15	-10 -78,-22 to 8,-66,-10	1112	.015 .012	4 -74 -14 -8 -70 -14	Vermal lobule VI L lobule VI	
5	-40 -42 -41	-48 -54 -46 to -34 -36 -36	808	.019 .011 .011	-38 -40 -40 -46 -48 -42 -46 -52 -44	L Crus II L Crus I L Crus II	Extends into VIIIb/VIII
<i>Alzheimer's disease</i>							
1	30 -71 -31	26 -78 -40 to 34 -62 -24	1144	.014	30 -68 -38	R Crus I, Crus II	
2	38 -61 -25	30 -66 -32 to 44 -58 -20	856	.015	40 -62 -24	R lobule VI, Crus I	
<i>Conjunction of age and Alzheimer's disease</i>							
1	36 -62 -27	30 -66 -32 to 40 -58 -22	408	.013	36 -62 -26	R lobule VI	Extends into Crus I
2	32 -72 -38		8	.008		Crus II	
3	30 -68 -30		8	.008		Crus I	

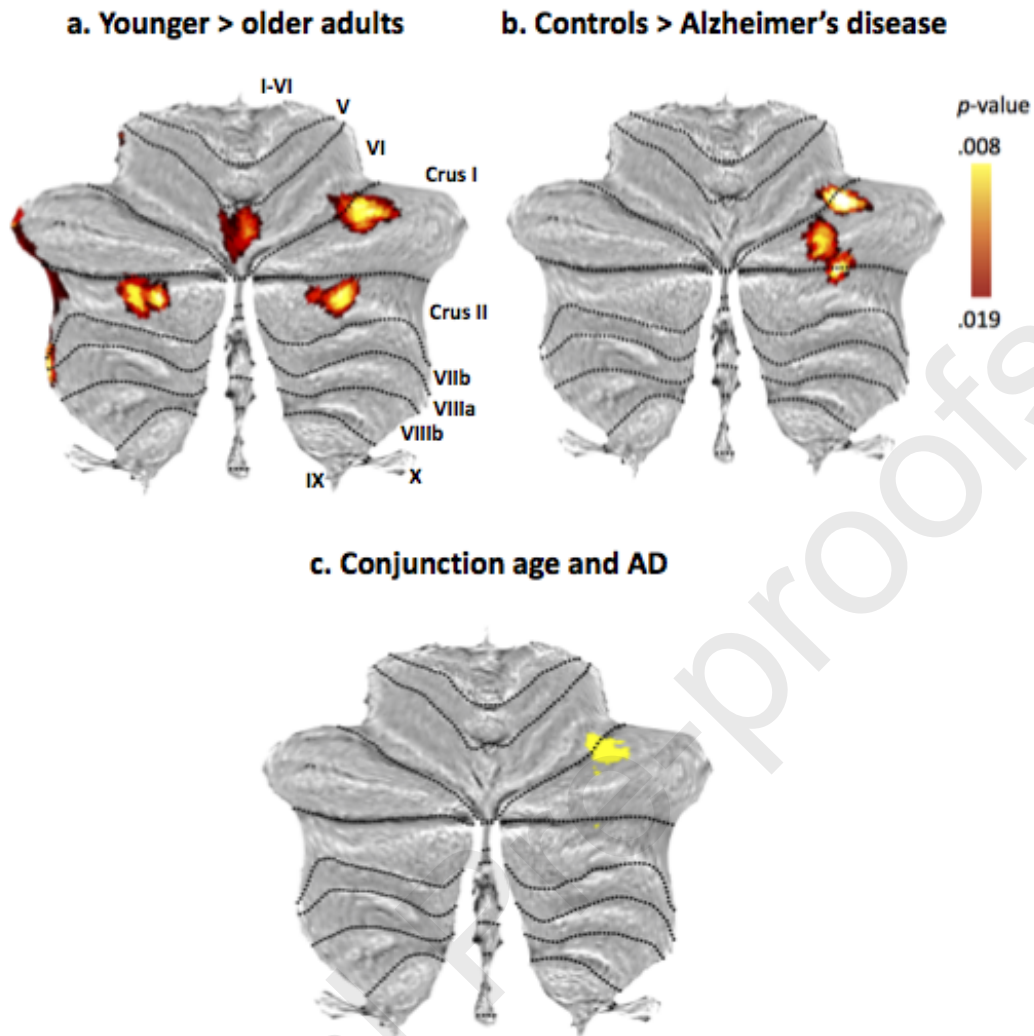


Figure 1. (a) Cerebellar grey matter loss in across 18 healthy ageing studies. (b) Cerebellar grey matter reductions in Alzheimer's disease across 13 studies. (c) Conjunction of effects of healthy ageing and Alzheimer's disease on grey matter volume. Note that these results are based on the voxelwise minimum value from the two input analyses on ageing and AD.

3.4 Placing our meta-analytic structural results in context with functional gradients and networks of the cerebellum

For plots comparing distributions of gradient values for each single gradient between age, AD and the AD-age overlap see Fig. 2. and Fig. 3 shows the distribution of gradient values colour-coded by functional brain network and flatmaps of gradient distributions with AD- and age-related atrophy clusters superimposed.

A comparison of the clusters of age-related grey matter reduction from our meta-analysis with the network connectivity patterns derived from Buckner and colleagues (Buckner et al., 2011) showed that the majority of age-related structural decline occurred in regions belonging to the frontoparietal and default mode networks (DMN), with some involvement of ventral and dorsal attention networks (Fig. 3). The voxels in the age-related grey matter loss clusters were involved in cognitive processing (tendency towards higher Gradient 1 values, $M=2.833$, $SD=3.630$) and encompassed both task-focused and task-unfocused domains (Gradient 2 mean value close to zero, $M=.055$, $SD=1.193$). Gradient 3 values for ageing included both minimum and maximum values, reflecting the distribution of age effects across the two hemispheres in cognitive territories of the cerebellar cortex ($M=-.144$, $SD=.652$). According to the overlap of age-related grey matter loss and the King et al. (2019) map, age-affected regions participate in working memory, attention, visual, affective and language processing.

The regions affected by AD also participate in DMN and the frontoparietal network. Higher Gradient 1 values highlight the involvement of cerebellar cognitive regions in this disease ($M=3.381$, $SD=2.427$), while motor regions are spared. The range of Gradient 2 values implicates both task-focused and unfocused processing regions in AD ($M=.220$, $SD=.929$). Gradient 3 values for AD were negative, reflecting the right lateralisation of grey matter decline ($M=-.604$, $SD=.228$). According to the overlap of age-related grey matter loss and the King et al. (2019) map, regions with AD-related grey matter atrophy participate in working memory, attention and language processing.

The ageing-AD conjunction voxels were located in regions that exhibit greater involvement in task-focused cognitive processes (high Gradient 2 values; $M=.995$,

$SD=1.193$; Fig. 3c). While grey matter loss in both AD and ageing involved DMN regions, all conjunction voxels overlapped with areas previously identified as belonging to the frontoparietal network (Buckner et al., 2011), in line with their role in cognitive control processes, such as divided attention and verbal fluency (King et al., 2019).

The distributions of Gradient 1 and 2 values in healthy ageing and AD were highly overlapping (Gradient 1: $Z=.320$, $p=.748$; Cohen's $U_I=.203$; Gradient 2: $Z=1.105$, $p=.272$; Cohen's $U_I=.084$; Fig. 2, 3). In contrast, regional grey matter loss due to healthy ageing was associated with higher median Gradient 3 values compared to AD-related structural decline ($Z=-10.549$, $p<.001$; Cohen's $U_I=.377$), reflecting the involvement of only the right (AD) as opposed to left and right (ageing) cerebellar hemispheres in each group. This finding could not be identified only based on macroscale brain network membership (DMN, FPN; Fig. 3d), but was reflected in the discrete functional mapping which suggested differences in the extent to which left and right hemispheres were involved in affective and language processing, respectively (Fig. 3e).

These findings regarding AD- and age-related cerebellar atrophy in regions of the DMN and FPN dovetail with cognitive deficits the included studies reported for older adults and AD patients, respectively. Across a variety of cognitive tasks, both healthy ageing and AD were associated with impairment in episodic and working memory as well as executive functioning (Appendix B, Table B1 for healthy ageing and Table B2 for AD). AD patients also exhibited deficits in verbal fluency. The studies on healthy ageing included here did not conduct further analyses to establish behavioural correlates of specific cerebellar regional grey matter decline. Among the few studies relating grey matter to clinical measures in AD, no correlation between

MMSE scores and cerebellar atrophy was found (Colloby, O'Brien, & Taylor, 2014; Farrow et al., 2007; Möller et al., 2013; Toniolo et al., 2018), but performance on figure copy tests was associated with volume of both anterior and posterior lobes (Toniolo et al., 2018).

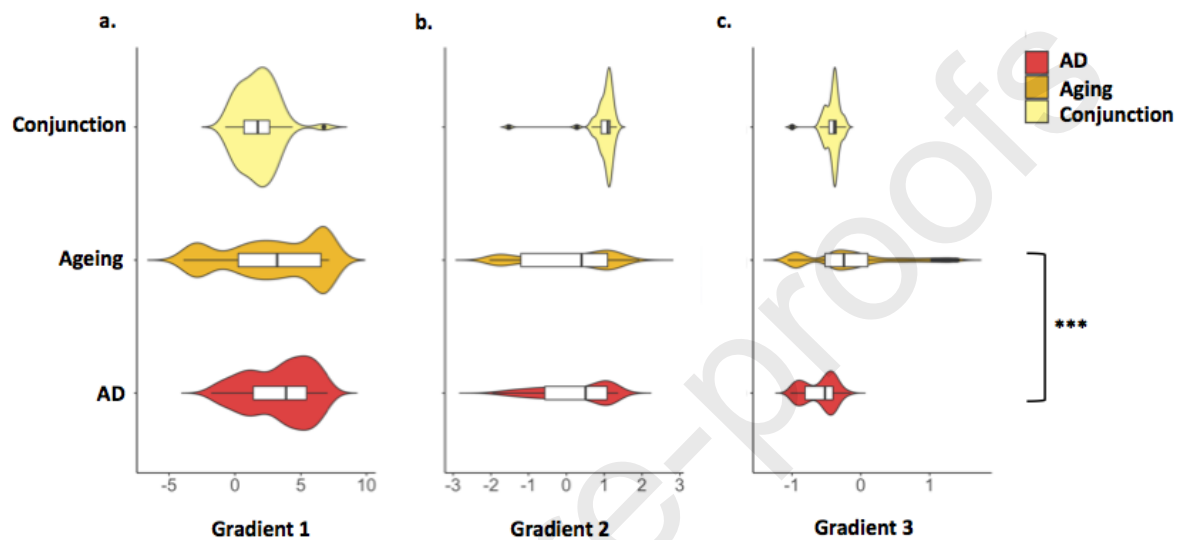
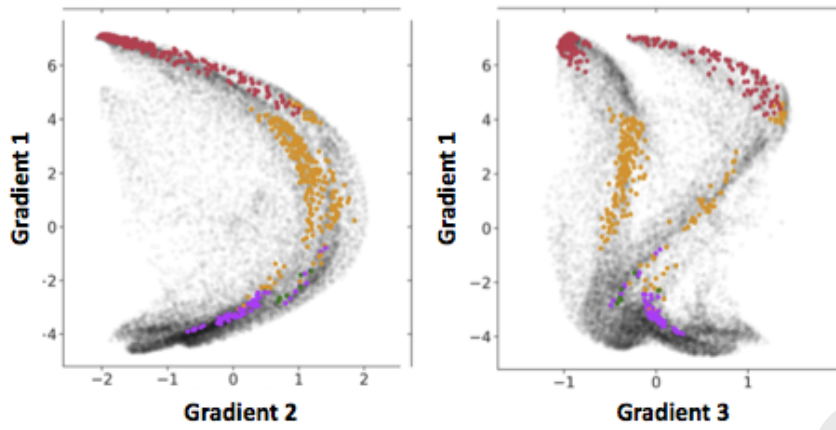


Figure 2. Violin plots showing the distribution of gradient values by analysis group.

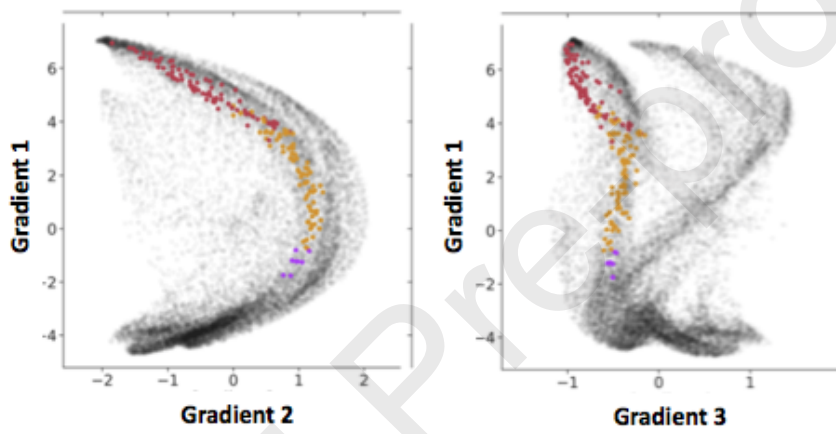
Permutations testing for differences in the rank sum of gradient values between healthy ageing and AD found no difference in Gradients 1 (a) and 2 (b) values. A significant difference in mean values was found for Gradient 3 (c) values.

*** $p < .001$

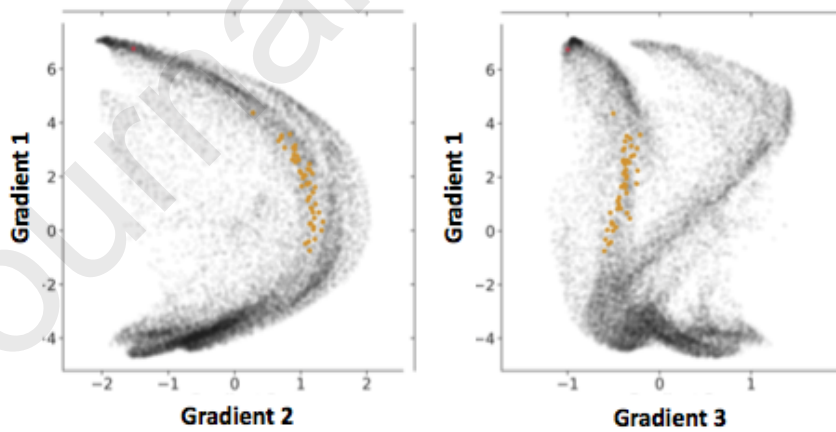
a. Healthy ageing



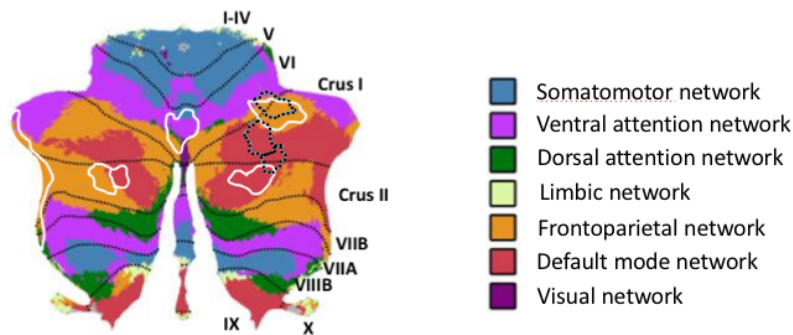
b. Alzheimer's disease



c. Conjunction of ageing and Alzheimer's disease



d. Intrinsic connectivity networks based on Buckner et al., 2011



e. Functional mapping based on King et al., 2019

1 Motor planning, left-hand presses, interference resolution

3 Visual working memory, saccades, visual letter recognition

5 Active maintenance, divided attention, mental arithmetic

7 Emotion processing, narrative, language processing

10 Visual letter recognition, autobiographical recall, interference resolution

2 Motor planning, right-hand presses, divided attention

4 Divided attention, action observation, motor planning

6 Active maintenance, divided attention, verbal fluency

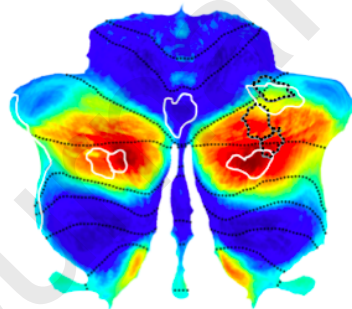
8 Language processing, word comprehension, narrative

9 Word comprehension, verbal fluency, mental arithmetic

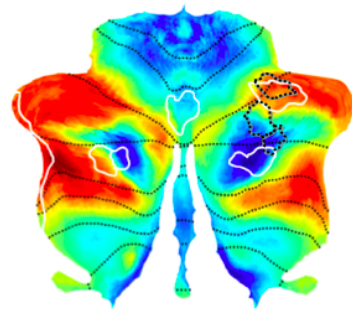


f. Continuous mappings of functional gradients based on Guell et al., 2018

Gradient 1: motor vs. cognitive processing



Gradient 2: degree of task focus



Gradient 3: hemispheric differences in cognitive processing

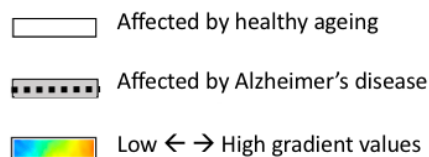
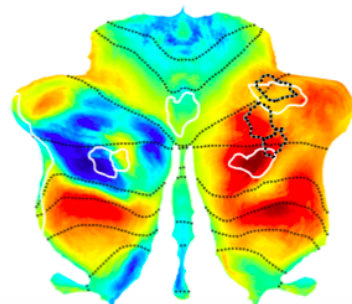


Figure 3. The distribution of the voxels of age-related grey matter loss according to the three main functional gradients of the cerebellum for (a) healthy ageing, (b) Alzheimer’s disease and (c) the conjunction of ageing and AD. Colour codes represent the intrinsic resting-state networks identified in Buckner et al. (2011) which are shown on a cerebellar flatmap in (d) (Diedrichsen and Zotow, 2015). (e) Task-based functional map of the cerebellum from King et al. (2019). (f) Gradient-based maps based on Guell et al. (2018). Gradient 1 represents the transition from motor tasks (lower values) to task-unfocused cognitive processing such as in the default mode network (higher values). Gradient 2 isolates attentional processing moving from task-unfocused (low values) to task-focused (high values) processes. Gradient 3 shows differences in lateralisation of non-motor processes. The regions with grey matter loss identified in our meta-analysis are plotted on top of each flatmap for healthy ageing (white outline) and Alzheimer’s disease (grey outline).

3.5 Robustness tests: jackknife analyses

The detailed results of each jackknife procedure are reported in Appendix D. For both the AD and ageing jackknife analyses there was no case in which removing one study from the analysis changed the label of the peak voxel of a cluster (Appendix D, Tables D1 and D2). Only slight shifts in peak voxel locations were observed. The jackknife procedure showed that healthy ageing clusters 1 and 2 in right Crus I/II were robust to the removal of any one study. Clusters 3 and 4 survived removal of all except one study each and remained stable in all other instances, indicating robustness in 94% of analyses. Cluster 5 in anterior Crus I/II remained stable in 83% of all analyses but did not survive correction for multiple comparisons upon removal of studies with a larger number of foci. For AD, there were two instances in which the removal of a study affected the survival of one of the two adjacent sub-clusters, but never both simultaneously. As a result, there was not a single jackknife analysis in which no AD-related atrophy occurred in the cerebellum

and each cluster was stable in 85% of analyses. In five jackknife analyses, Clusters 1 and 2 merged into one larger cluster without resulting in substantial shifts in the locations of cluster peaks.

On average across all jackknife analyses, Gradient 1 and 2 values were not significantly different between healthy ageing and AD. The significant difference in Gradient 3 between ageing and AD remained in all leave-one-out analyses. In all jackknife analyses, age- and AD-related regions were part of the DMN and FPN networks and were involved in cognitive control and language processing, demonstrating the stability of the functional mappings of regions with AD- and age-dependent grey matter loss.

4. Discussion

4.1 General Discussion

We aimed to determine whether Alzheimer's disease and normal ageing result in dissociable patterns of cerebellar grey matter loss and whether the functional profile of the affected regions could be differentiated. To answer these questions, we employed anatomical likelihood estimation (ALE) meta-analysis to identify consistent patterns of cerebellar grey matter atrophy across 18 studies of healthy ageing. We further compared age-related decline to that observed in 13 studies of Alzheimer's disease. Age and AD exhibited grey matter decline in posterior cerebellum in Crus I/II and lobule VI, albeit in largely non-overlapping subregions of these lobules. The most striking finding was the strict right lateralisation of grey matter loss in AD compared to bilateral decline in healthy ageing.

We used three complimentary mappings of the cerebellum to characterise the functional profile of the regions with grey matter loss in ageing and AD: the known intrinsic brain networks based on resting state fMRI (Buckner et al., 2011), the task-based mapping with discrete functional boundaries (King et al., 2019), and a multi-dimensional continuous map reflecting the three major gradients that govern the functional organisation of the cerebellum (cognitive to motor, degree of task focus, and qualitative differences in left and right homologues of posterior cognitive cerebellum; Guell, Schmahmann, Gabrieli, et al., 2018). Using the gradient-based approach in combination with structural findings allowed a more nuanced characterisation of vulnerable cerebellar regions, over and above discrete or categorical descriptions of their function. It also allowed for a statistical quantification of differences in functional preferences between AD- and age-affected regions.

Despite only a small spatial overlap of regions with age- and AD-related cerebellar grey matter loss, both exhibit a strong bias towards cognitive as opposed to motor processing (Gradient 1) and involvement across the task-focused to unfocused continuum (Gradient 2; Guell, Schmahmann, Gabrieli, et al., 2018). This was also in line with the role of these regions in default mode and frontoparietal networks (Buckner et al., 2011), as well as many shared functional characteristics suggesting their involvement in working memory, attention, and language processing (King et al., 2019).

Notwithstanding these functional similarities, regions affected by normal ageing and AD also showed some differences in their functional characterisation. Specifically, they held different positions along the third gradient. Gradient 3 highlights differences that exist in cognitive processing in the two hemispheres but are not present in motor domains. Note that the interpretation of Gradient 3 values

does not simply pertain to spatial localisation of a cluster to the left or right hemisphere. In fact, Gradient 3 reflects higher lateralisation of cognitive functions as opposed to primary motor functions. The same regions in left and right homologues of the motor cerebellum (lobules IV-VIII) would be described with the same gradient values. However, left and right hemispheric areas of nonmotor processing (lobules Crus I/II, VIIb, IX) lie on two opposing ends of the spectrum (Guell et al., 2018).

These findings suggest that regions with grey matter loss in ageing and AD do not only reflect differences in spatial localisation to the left and right hemispheres, but also qualitative differences in the functions carried out by the left and right homologues of posterior cerebellar cortex. They point to a dissociation between the functional connectivity fingerprint of the two homologues of posterior cerebellar lobules and highlight their differential vulnerability to AD and age, respectively. In contrast, the intrinsic functional connectivity networks based on resting-state fMRI grouped both regions into the same networks (frontoparietal and default mode; Buckner et al., 2011). The gradient findings provide a complementary statistical confirmation of the picture obtained from the King et al. (2019) map. This map also suggests laterality differences where the right posterior cerebellar hemisphere holds a more prominent role in verbal processing (especially Crus I/II), while only the left region seems to be involved in emotional processes.

4.2 Prior evidence of macroscale cerebellar changes in healthy ageing and AD: implications for behaviour

Dominant views on the role of cerebellar function in cognitive, motor and affective processes postulate that the striking uniformity of cerebellar micro-circuitry suggests that a single computational mechanism, the “universal cerebellar transform”,

operates on inputs from extra-cerebellar structures involved across behavioural domains (Schmahmann, 2000). The cerebellum is thought to aid behaviour by learning from external input and forming internal models for automatic processing and more efficient behaviour (Balsters & Ramnani, 2011). Functional specialisation would therefore be dictated by the connectivity profile of a given cerebellar subregion (Guell et al., 2018). As a result, detrimental effects of grey matter loss should be region-specific and can affect a variety of different functional domains by virtue of poorer modulation of behaviour as the communication between cerebellum and neocortical and limbic regions is impaired (Jacobs et al., 2018).

Prior research and our findings suggest that age- and AD-related changes in multiple cerebellar subregions also impact multiple functional domains, especially those supporting cognitive processes (Gellersen et al., 2017). In posterior cerebellar regions, grey matter volume loss has been associated with performance on a variety of cognitive functions in healthy older adults and AD many of which co-localise with regions in our meta-analysis (Bernard & Seidler, 2014; Jacobs et al., 2018; Thomann et al., 2008). This can even be found when controlling for cerebral cortical or hippocampal volume, strongly suggesting an independent contribution to cognitive status in ageing and AD (Buhrmann et al., 2020; Lin, Chen, Tom, & Kuo, 2020).

A finding unique to the ageing as opposed to the AD data was a cluster in a cerebellar region of the DMN that may contribute to emotion processing (King et al., 2019). Despite its well established role in affective symptoms across a range of neuropsychiatric disorders (Schmahmann, 2004), we are only aware of one study that linked the volume of the same Crus II region and its cortical connectivity pattern with altered emotional processing in healthy older adults (Uwisengeyimana et al., 2020).

More common in the healthy ageing literature are positive associations between grey matter volume of the cerebellum and executive functioning, memory and language processing: long-term memory performance is related to larger total cerebellar volume and lobules VI and Crus II (Becker et al., 2015; Hafkemeijer et al., 2014; Koppelmans et al., 2017; Serra et al., 2017); posterior cerebellar volume, especially Crus II, is associated with scores on language tasks (Rodríguez-Aranda et al., 2016); and the most frequent association between cerebellar volume and cognition can be observed for tasks involving executive functions and processing speed, most notably in lobule VI and Crus I (Buhrmann et al., 2020; Koini et al., 2018; Liang & Carlson, 2019; Ruscheweyh et al., 2013; Uwisengeyimana et al., 2020; Zhang et al., 2013). These findings are therefore in line with the functional mappings we used here and mostly dovetail with our results in that age-related grey matter loss was found in cognitive cerebellar regions involved in DMN, FPN and attention networks.

Recent data have shown age differences in cerebellar engagement across cognitive domains including lobule VI and Crus I/II (Bernard et al., 2020) and differences in cerebral-cerebellar connectivity (Bernard & Seidler, 2014). The authors hypothesise that fewer cerebellar resources reduce the support of automatic processes based on internal behavioural models (Bernard et al., 2020). Under-activation of posterior regions situated in FPN (Bernard et al., 2020) and the grey matter loss observed here in the same areas may contribute to a reduction in efficiency of cerebellar recruitment during cognitive tasks. Without longitudinal data, it remains unclear whether these changes in cerebellar engagement and neocortical-cerebellar connectivity are a result of grey matter loss or whether the opposite is the case. Future studies might examine whether decreases in grey matter in the regions identified here are driving such changes in BOLD activation.

Similarly to the functional mappings for healthy ageing, AD-related cerebellar grey matter loss occurred in Crus I/II and lobule VI. However, for AD this was only the case in the right hemisphere. These regions lie on the cognitive extreme of the cognitive-motor gradient but show no preference along the gradient measuring task positivity, in line with their participation in both default mode and frontoparietal networks (Buckner et al., 2011; Guell et al., 2018). Previous studies on cerebellar grey matter volume and its association with cognition in AD have found deficits in those functions that map onto the regions we identified as most vulnerable to AD-related atrophy: language and attentional processes, as well as cognitive control of memory retrieval and other executive functions, including processing speed and working memory (Arnaiz & Almkvist, 2003; Baldaçara et al., 2011; Dos Santos et al., 2011; Hoche, Guell, Vangel, Sherman, & Schmahmann, 2018; Lin et al., 2020; Thomann et al., 2008; Toniolo et al., 2018). It is of note that there are also multiple occasions on which standard neuropsychological dementia screening tools of global cognition (such as the Mini Mental State Exam or the ADAS-Cog) are unrelated to cerebellar volume (Colloby, O'Brien, et al., 2014; Farrow et al., 2007; Lin et al., 2020; Möller et al., 2013; Toniolo et al., 2018). One explanation may be that cerebellar grey matter loss can still be compensated in earlier stages of the disease. Another reason that is likely is that these standard tools do not assess specific cognitive functions in depth, collapse scores across domains and therefore do not tap into the specific functions supported by the cerebellum (Hoxha et al., 2018).

Grey matter loss as observed in our meta-analysis may contribute to the altered connectivity between hippocampus, cerebral, and cerebellar DMN regions already seen in early AD, individuals with mild cognitive impairment (MCI) and even healthy older adults with subjective memory complaints (Bai et al., 2009; Greicius et

al., 2004; Hafkemeijer et al., 2013; Serra et al., 2017). This may result in a reduction in efficient communication with neocortical and limbic regions which impacts cognitive performance (Liang & Carlson, 2019). Even the strongest genetic risk factor for AD (the epsilon-4 allele of the apolipoprotein gene) has been shown to affect cerebellar communication with corticolimbic regions during memory tasks in young e4-carriers (Matura et al., 2014). These functional effects in young e4-carriers bore a striking resemblance with the cluster in right Crus I/lobule VI that we identified here and may be a precursor to obvious grey matter and cognitive decline in later disease stages.

There is mixed evidence with respect to the vulnerability of the cerebellum to amyloid beta. Some argue that the cerebellum is mostly resistant to amyloid pathology until later stages of Alzheimer's disease (Liang & Carlson, 2019). Others counter that AD pathology affects the cerebellum even in early stages leading to both motor and cognitive deficits in mouse models (Hoxha et al., 2018; Jacobs et al., 2018). AD pathology is likely to be related to cerebellar atrophy, as amyloid beta correlates with grey matter in the cerebellum even among healthy older adults (Oh, Madison, Villeneuve, Markley, & Jagust, 2014) and cerebellar volume loss occurs in both sporadic and early-onset AD (Gellersen et al., 2017; Guo et al., 2016a; Jacobs et al., 2018). It has been suggested that one reason for prior absence of amyloid pathology in the cerebellum may be methodological limitations in staining techniques, rather than a true resistance (Jacobs et al., 2018). As a result, the cerebellum may have been under-researched and used as a reference region in PET imaging, precluding further findings of AD pathology in patients. Multiple reviews dovetail with our findings that the cerebellum still plays a role in AD (Gellersen et al., 2017; Jacobs et al., 2018; Lin et al., 2020).

Longitudinal studies that could track the evolution of cerebellar volume and function across the AD-continuum are needed to better understand the role of the cerebellum in functional decline and its interplay with other brain areas. Differential subregional vulnerability to AD pathology or to normal ageing may be due to downstream influences resulting from cerebro-cerebellar synergism (Raz & Rodrigue, 2006; Sullivan & Pfefferbaum, 2006). Structural decline in the cerebellum may also have selective effects on distant neocortical regions (Guo et al., 2016b; Hogan et al., 2011; Limperopoulos, Chilingaryan, Guizard, Robertson, & Du Plessis, 2010). Recent studies on longitudinal changes in cerebellar volume in AD have come to conflicting results, with one suggesting that cerebellar volume loss only contributes to disease progression in later stages from MCI to AD (Tabatabaei-Jafari, Walsh, Shaw, & Cherbuin, 2017), whereas another stipulates that the opposite is true (Lin et al., 2020). Both studies only consider total cerebellar volume and did not relate changes in grey matter to changes in cognition between baseline and follow-up. A mechanistic understanding of the cerebellum's role in AD is therefore still lacking.

4.3 Limitations and future directions

It is surprising that we did not find clusters of significant age-related grey matter loss in anterior motor regions of the cerebellum. Prior evidence has shown volumetric decline of motor regions in normal ageing which correlates with motor deficits (Bernard et al., 2015; Bernard & Seidler, 2013; Hulst et al., 2015; Koppelmans et al., 2017; Liang & Carlson, 2019; Uwisengeyimana et al., 2020). However, some of these and other studies assessed in our literature search did not include coordinates of grey matter loss and could not be used in the present meta-analysis. Our analysis likely underestimates the extent of grey matter reductions in the

cerebellum in healthy ageing and should not be interpreted as a demonstration of the absence of an age effect on cerebellar motor regions. Replication based on data from single subjects is an important next step.

It should be noted though, that this apparent limitation of the coordinate-based meta-analysis also presents an advantage. Our meta-analytic method does not require lobular boundaries as a constraint, which would be detrimental to the interpretation of functional implications given that anatomical borders do not translate neatly to boundaries between functional domains (King et al., 2019). These recent parcellations demonstrate that the mere knowledge of the lobule in which grey matter atrophy occurs may be too simplistic for the characterisation of function. Previous volumetry studies likely combine distinct functional territories which may obscure volume-function relationships. Especially those studies focusing on total grey matter volume cannot further our understanding of the precise role of regional cerebellar grey matter loss for specific cognitive changes in ageing or AD (Lin et al., 2020; Tabatabaei-Jafari et al., 2017).

Given that the majority of AD studies in our analysis included mild to moderate AD cases, we could not run subgroup analyses based on disease severity. We would expect, however, that grey matter atrophy in AD occurs in a network-based fashion (Guo et al., 2016b): posterior cerebellar regions connected to medial temporal lobe with earliest tau and parietal regions with the earliest amyloid beta deposition are affected first (Braak & Braak, 1995; Insel, Mormino, Aisen, Thompson, & Donohue, 2020), and anterior cerebellar regions follow (although note that in some cases anterior cerebellar atrophy can also be found in early stages; Toniolo et al., 2018). This would dovetail with our findings of AD-related atrophy in DMN and FPN.

As discussed above, prior studies and our findings converged to point to right regions of lobule VI and Crus I/II as particularly vulnerable to age, AD genetic risk and actual AD cases. AD may exacerbate the downward trajectory of this region already observed in healthy ageing shown here. Alternatively, the studies that found significant age-related grey matter loss in these regions may point out early declines that will later manifest as AD. Our data are limited in that they cannot test this possibility given the lack of longitudinal data in our analysis.

It is not clear to what extent cerebellar structural decline has clinical relevance for behavioural deficits in AD patients. As mentioned above, cerebellar deficits alone may not be sufficient to result in scores below the cut-off point for normal functioning in standard AD screenings because they are masked by the large number of test items that are insensitive to cerebellar function (Hoche et al., 2018). It is possible that correlations between cerebellar grey matter and affective-cognitive functioning in AD may be detected more readily with a more sensitive tool geared towards deficits caused by cerebellar decline, such as the novel Cerebellar Cognitive Affective/Schmahmann Syndrome Scale (Hoche et al., 2018). This may be an interesting avenue for future research.

Finally, our findings may be of relevance for studies aiming to determine optimal targets for neuromodulatory therapeutic approaches in ageing and AD. Non-invasive modulation of cerebellar regions has been shown to have network- and task-specific effects on connected neocortical regions (D'Mello, Turkeltaub, & Stoodley, 2017; Halko, Farzan, Eldaief, Schmahmann, & Pascual-Leone, 2014). Targeting cerebellar regions that are part of cortico-limbic networks most affected by AD through augmentative neuromodulation may bolster long-range connectivity.

4.4 Conclusions

Structural and functional analyses combined paint a picture of divergent and convergent patterns of cerebellar vulnerability to age and AD. The meta-analysis highlights vulnerability of posterior cerebellum to AD and ageing (Crus I/II, lobule VI), suggesting that some aspects of the age-related downward trajectory of grey matter may be exacerbated by AD pathology. The strict right lateralisation of AD atrophy compared to bilateral effects in healthy ageing was striking. Notably, besides being located in the same lobules, the subregions of structural atrophy for AD and ageing were mainly non-overlapping. Nonetheless, regions with vulnerability to AD and ageing exhibited similar functional profiles: they participated in the same large-scale discrete functional networks, were involved in working memory, attention and language processing, and were located in similar positions along major functional gradients (cognitive vs. motor and degree of task focus). Despite these similarities, differences along Gradient 3 allowed for the observation of age-AD divergence along alternative dimensions of cerebellar functional hierarchies as exemplified by different preferences along the tertiary cerebellar gradient (lateralisation in cognitive territories) and showed that only regions with age-related grey matter decline were involved in affective processes. These findings show subtler differences in the functional fingerprint of regions impacted by AD and ageing that the standard categorical parcellations of brain networks was not able to detect. Our study provides an unprecedented characterisation of structural and functional localisation differences and similarities in cerebellar atrophy between ageing and AD. They also show how the use of multiple functional maps of the cerebellum is synergistic in interpreting the implications of regional grey matter loss. More research is needed to better understand 1) how age and pathology impact cerebellar computational processes, 2)

how cerebellar interactions with other brain regions may influence cognitive decline or preservation in healthy ageing and AD, 3) and the role of subregional cerebellar grey matter loss in the neuropsychology of AD.

References

- Ahmed, R. M., Landin-Romero, R., Liang, C. T., Keogh, J. M., Henning, E., Strikwerda-Brown, C., ... Piguet, O. (2019). Neural networks associated with body composition in frontotemporal dementia. *Annals of Clinical and Translational Neurology*, 6(9), 1707–1717. <https://doi.org/10.1002/acn3.50869>
- Arnaiz, E., & Almkvist, O. (2003). Neuropsychological features of mild cognitive impairment and preclinical Alzheimer's disease. *Acta Neurologica Scandinavica*, 107(s179), 34–41. <https://doi.org/10.1034/j.1600-0404.107.s179.7.x>
- Bai, F., Zhang, Z., Watson, D. R., Yu, H., Shi, Y., Yuan, Y., ... Qian, Y. (2009). Abnormal Functional Connectivity of Hippocampus During Episodic Memory Retrieval Processing Network in Amnesic Mild Cognitive Impairment. *Biological Psychiatry*, 65(11), 951–958. <https://doi.org/10.1016/j.biopsych.2008.10.017>
- Baldaçara, L., Borgio, J. G. F., Moraes, W. A. dos S., Lacerda, A. L. T., Montaña, M. B. M. M., Tufik, S., ... Jackowski, A. P. (2011). Cerebellar volume in patients with dementia. *Revista Brasileira de Psiquiatria*, 33(2), 122–129. <https://doi.org/10.1590/S1516-44462011005000012>
- Balsters, J. H., & Ramnani, N. (2011). Cerebellar plasticity and the automation of first-order rules. *Journal of Neuroscience*, 31(6), 2305–2312. <https://doi.org/10.1523/JNEUROSCI.4358-10.2011>
- Becker, N., Laukka, E. J., Kalpouzos, G., Naveh-Benjamin, M., Bäckman, L., & Brehmer, Y. (2015). Structural brain correlates of associative memory in older adults. *NeuroImage*, 118, 146–153. <https://doi.org/10.1016/j.neuroimage.2015.06.002>
- Bernard, J. A., Leopold, D. R., Calhoun, V. D., & Mittal, V. A. (2015). Regional Cerebellar Volume and Cognitive Function From Adolescence to Late Middle Age. *Human Brain Mapping*, 36(3), 1102–1120. <https://doi.org/10.1002/hbm.22690.Regional>
- Bernard, J. A., Nguyen, A. D., Hausman, H. K., Maldonado, T., Ballard, H. K., Eakin, S. M., ... Goen, J. R. M. M. (2020). Shaky scaffolding: Age differences in cerebellar activation revealed through activation likelihood estimation meta-analysis. *Human Brain Mapping*, (May), 1–27. <https://doi.org/10.1002/hbm.25191>
- Bernard, J. A., & Seidler, R. D. (2013). Relationships between regional cerebellar volume and sensorimotor and cognitive function in young and older adults. *Cerebellum*, 12(5), 721–737. <https://doi.org/10.1007/s12311-013-0481-z>
- Bernard, J. A., & Seidler, R. D. (2014). Moving forward: Age effects on the cerebellum underlie cognitive and motor declines. *Neuroscience and Biobehavioral Reviews*, 42, 193–207. <https://doi.org/10.1016/j.neubiorev.2014.02.011>
- Braak, H., & Braak, E. (1995). Staging of Alzheimer's Disease-Related Neurofibrillary Changes. *Neurobiology of Aging*, 16(3), 271–284.

- Buckner, R. L., Krienen, F. M., Castellanos, A., Diaz, J. C., & Yeo, B. T. T. (2011). The organization of the human cerebellum estimated by intrinsic functional connectivity. *Journal of Neurophysiology*, *106*(5), 2322–2345. <https://doi.org/10.1152/jn.00339.2011>
- Buhrmann, A., Brands, A. M. A., van der Grond, J., Schilder, C., van der Mast, R. C., Ottenheim, N. R., ... van den Berg, E. (2020). Cerebellar Grey Matter Volume in Older Persons Is Associated with Worse Cognitive Functioning. *Cerebellum*, *i*. <https://doi.org/10.1007/s12311-020-01148-0>
- Cohen, J. (1988). *Statistical power analysis for the behavioral sciences* (2nd ed.; Lawrence Erlbaum, ed.). Hillsdale, N.J.: New York: Academic Press.
- Colloby, S. J., O'Brien, J. T., & Taylor, J. P. (2014). Patterns of cerebellar volume loss in dementia with Lewy bodies and Alzheimer's disease: A VBM-DARTEL study. *Psychiatry Research - Neuroimaging*, *223*(3), 187–191. <https://doi.org/10.1016/j.psychres.2014.06.006>
- Colloby, S. J., O'Brien, J. T., Taylor, J.-P. P., O'Brien, J. T., Taylor, J.-P. P., O'Brien, J. T., & Taylor, J.-P. P. (2014). Patterns of cerebellar volume loss in dementia with Lewy bodies and Alzheimer's disease: A VBM-DARTEL study. *Psychiatry Research - Neuroimaging*, *223*(3), 187–191. <https://doi.org/http://dx.doi.org/10.1016/j.psychres.2014.06.006>
- D'Mello, A. M., Turkeltaub, P. E., & Stoodley, C. J. (2017). Cerebellar tDCS Modulates Neural Circuits during Semantic Prediction: A Combined tDCS-fMRI Study. *The Journal of Neuroscience*, *37*(6), 1604–1613. <https://doi.org/10.1523/jneurosci.2818-16.2017>
- Diedrichsen, J., Balsters, J. H., Flavell, J., Cussans, E., & Ramnani, N. (2009). A probabilistic MR atlas of the human cerebellum. *NeuroImage*, *46*(1), 39–46. <https://doi.org/10.1016/j.neuroimage.2009.01.045>
- Diedrichsen, J., Maderwald, S., Küper, M., Thürling, M., Rabe, K., Gizewski, E. R., ... Timmann, D. (2011). Imaging the deep cerebellar nuclei: A probabilistic atlas and normalization procedure. *NeuroImage*, *54*(3), 1786–1794. <https://doi.org/10.1016/j.neuroimage.2010.10.035>
- Diedrichsen, J., & Zotow, E. (2015). Surface-based display of volume-averaged cerebellar imaging data. *PLoS ONE*, *10*(7), 1–18. <https://doi.org/10.1371/journal.pone.0133402>
- Dos Santos, V., Thomanna, P. A., Wüstenberg, T., Seidl, U., Essig, M., & Schröder, J. (2011). Morphological cerebral correlates of CERAD test performance in mild cognitive impairment and Alzheimer's disease. *Journal of Alzheimer's Disease*, *23*(3), 411–420. <https://doi.org/10.3233/JAD-2010-100156>
- Eickhoff, S. B., Bzdok, D., Laird, A. R., Kurth, F., & Fox, P. T. (2012). Activation likelihood estimation revisited. *NeuroImage*, *59*(3), 2349–2361. <https://doi.org/10.1016/j.neuroimage.2011.09.017>
- Eickhoff, S. B., Bzdok, D., Laird, A. R., Roski, C., Caspers, S., Zilles, K., & Fox, P. T. (2011). Co-activation patterns distinguish cortical modules, their connectivity and functional differentiation. *NeuroImage*, *57*(3), 938–949. <https://doi.org/10.1016/j.neuroimage.2011.05.021>
- Eickhoff, S. B., Laird, A. R., Grefkes, C., Wang, L. E., Zilles, K., & Fox, P. T. (2009). Coordinate-based activation likelihood estimation meta-analysis of neuroimaging data: A random-effects approach based on empirical estimates of spatial uncertainty. *Human Brain Mapping*, *30*(9), 2907–2926. <https://doi.org/10.1002/hbm.20718>
- Eickhoff, S. B., Nichols, T. E., Laird, A. R., Hoffstaedter, F., Amunts, K., Fox, P. T.,

- ... Eickhoff, C. R. (2016). NeuroImage Behavior, sensitivity, and power of activation likelihood estimation characterized by massive empirical simulation. *NeuroImage*, *137*, 70–85. <https://doi.org/10.1016/j.neuroimage.2016.04.072>
- Farrow, T. F. D., Thiyaresh, S. N., Wilkinson, I. D., Parks, R. W., Ingram, L., & Woodruff, P. W. R. (2007). Fronto-temporal-lobe atrophy in early-stage Alzheimer's disease identified using an improved detection methodology. *Psychiatry Res*, *155*(1), 11–19. <https://doi.org/10.1016/j.psychres.2006.12.013>
- Gellersen, H. M., Guo, C. C., O'Callaghan, C., Tan, R. H., Sami, S., & Hornberger, M. (2017). Cerebellar atrophy in neurodegeneration - a meta-analysis. *Journal of Neurology, Neurosurgery and Psychiatry*, *88*(9). <https://doi.org/10.1136/jnnp-2017-315607>
- Greicius, M. D., Srivastava, G., Reiss, A. L., Menon, V., Raichle, E., Greicius, M. D., ... Menon, V. (2004). Default-Mode Network Activity Distinguishes Alzheimer's Disease from Healthy Aging: Evidence from Functional MRI. *Proceedings of the National Academy of Sciences*, *101*(13), 4637–4642.
- Guell, X., Goncalves, M., Kaczmarzyk, J. R., Gabrieli, J. D. E. E., Schmahmann, J. D., & Ghosh, S. S. (2019). Littlebrain: A gradient-based tool for the topographical interpretation of cerebellar neuroimaging findings. *PLoS ONE*, *14*(1), 1–16. <https://doi.org/10.1371/journal.pone.0210028>
- Guell, X., Schmahmann, J. D., Gabrieli, J. D. E. DE, & Ghosh, S. S. (2018). Functional gradients of the cerebellum. *ELife*, *7*, 1–22. <https://doi.org/10.7554/elife.36652>
- Guo, C. C., Tan, R., Hodges, J. R., Hu, X., Sami, S., & Hornberger, M. (2016a). Network-selective vulnerability of the human cerebellum to Alzheimer's disease and frontotemporal dementia. *Brain*, *139*, 1527–1538. <https://doi.org/10.1093/brain/aww003>
- Guo, C. C., Tan, R., Hodges, J. R., Hu, X., Sami, S., & Hornberger, M. (2016b). Network-selective vulnerability of the human cerebellum to Alzheimer's disease and frontotemporal dementia. *Brain*, *139*(5), 1527–1538. <https://doi.org/10.1093/brain/aww003>
- Hafkemeijer, A., Altmann-Schneider, I., de Craen, A. J. M., Slagboom, P. E., van der Grond, J., & Rombouts, S. A. R. B. (2014). Associations between age and gray matter volume in anatomical brain networks in middle-aged to older adults. *Aging Cell*, *13*(6), 1068–1074. <https://doi.org/10.1111/accel.12271>
- Hafkemeijer, A., Altmann-Schneider, I., Oleksik, A. M., van de Wiel, L., Middelkoop, H. A. M. M., van Buchem, M. A., ... Rombouts, S. A. R. B. R. B. (2013). Increased functional connectivity and brain atrophy in elderly with subjective memory complaints. *Brain Connectivity*, *3*(4), 353–362. <https://doi.org/10.1089/brain.2013.0144>
- Halko, M. A., Farzan, F., Eldaief, M. C., Schmahmann, J. D., & Pascual-Leone, A. (2014). Intermittent Theta-Burst Stimulation of the Lateral Cerebellum Increases Functional Connectivity of the Default Network. *Journal of Neuroscience*, *34*(36), 12049–12056. <https://doi.org/10.1523/JNEUROSCI.1776-14.2014>
- Hentschke, H., & Stüttgen, M. C. (2011). Computation of measures of effect size for neuroscience data sets. *European Journal of Neuroscience*, *34*(12), 1887–1894. <https://doi.org/10.1111/j.1460-9568.2011.07902.x>
- Hoche, F., Guell, X., Vangel, M. G., Sherman, J. C., & Schmahmann, J. D. (2018). The cerebellar cognitive affective/Schmahmann syndrome scale. *Brain*, *141*(1), 248–270. <https://doi.org/10.1093/brain/awx317>

- Hogan, M. J., Staff, R. T., Bunting, B. P., Murray, A. D., Ahearn, T. S., Deary, I. J., & Whalley, L. J. (2011). Cerebellar brain volume accounts for variance in cognitive performance in older adults. *Cortex*, *47*(4), 441–450. <https://doi.org/10.1016/j.cortex.2010.01.001>
- Hoxha, E., Lippiello, P., Zurlo, F., Balbo, I., Santamaria, R., Tempia, F., & Miniaci, M. C. (2018). The emerging role of altered cerebellar synaptic processing in Alzheimer's disease. *Frontiers in Aging Neuroscience*, *10*(November), 1–9. <https://doi.org/10.3389/fnagi.2018.00396>
- Hulst, T., van der Geest, J. N., Thürling, M., Goericke, S., Frens, M. A., Timmann, D., & Donchin, O. (2015). Ageing shows a pattern of cerebellar degeneration analogous, but not equal, to that in patients suffering from cerebellar degenerative disease. *NeuroImage*, *116*, 196–206. <https://doi.org/10.1016/j.neuroimage.2015.03.084>
- Insel, P. S., Mormino, E. C., Aisen, P. S., Thompson, W. K., & Donohue, M. C. (2020). Neuroanatomical spread of amyloid β and tau in Alzheimer's disease: implications for primary prevention. *Brain Communications*, *2*(1), 1–11. <https://doi.org/10.1093/braincomms/fcaa007>
- Jacobs, H. I. L., Hopkins, D. A., Mayrhofer, H. C., Bruner, E., Van Leeuwen, F. W., Raaijmakers, W., & Schmahmann, J. D. (2018). The cerebellum in Alzheimer's disease: Evaluating its role in cognitive decline. *Brain*, *141*(1), 37–47. <https://doi.org/10.1093/brain/awx194>
- Jernigan, T. L., Archibald, S. L., Fennema-Notestine, C., Gamst, A. C., Stout, J. C., Bonner, J., & Hesselink, J. R. (2001). Effects of age on tissues and regions of the cerebrum and cerebellum. *Neurobiology of Aging*, *22*(4), 581–594. [https://doi.org/10.1016/S0197-4580\(01\)00217-2](https://doi.org/10.1016/S0197-4580(01)00217-2)
- Kelly, R. M., & Strick, P. L. (2003). Cerebellar loops with motor cortex and prefrontal cortex of a nonhuman primate. *Journal of Neuroscience*, *23*(23), 8432–8444. Retrieved from <https://www.ncbi.nlm.nih.gov/pubmed/12968006>
- King, M., Hernandez-Castillo, C. R., Poldrack, R. A., Ivry, R. B., & Diedrichsen, J. (2019). Functional boundaries in the human cerebellum revealed by a multi-domain task battery. *Nature Neuroscience*, *22*(8), 1371–1378. <https://doi.org/10.1038/s41593-019-0436-x>
- Koini, M., Duering, M., Gesierich, B. G., Rombouts, S. A. R. B., Ropele, S., Wagner, F., ... Schmidt, R. (2018). Grey-matter network disintegration as predictor of cognitive and motor function with aging. *Brain Structure & Function*, *223*(5), 2475–2487. <https://doi.org/10.1007/s00429-018-1642-0>
- Koppelmans, V., Hoogendam, Y. Y., Hirsiger, S., Mérrillat, S., Jäncke, L., Seidler, R. D., ... Seidler, R. D. (2017). Regional cerebellar volumetric correlates of manual motor and cognitive function. *Brain Structure and Function*, *222*(4), 1929–1944. <https://doi.org/10.1007/s00429-016-1317-7>
- Laird, A. R., Fox, P. M., Price, C. J., Glahn, D. C., Uecker, A. M., Lancaster, J. L., ... Fox, P. T. (2005). ALE meta-analysis: Controlling the false discovery rate and performing statistical contrasts. *Human Brain Mapping*, *25*(1), 155–164. <https://doi.org/10.1002/hbm.20136>
- Liang, K. J., & Carlson, E. S. (2019). Resistance, vulnerability and resilience: A review of the cognitive cerebellum in aging and neurodegenerative diseases. *Neurobiology of Learning and Memory*, (September 2018), 0–1. <https://doi.org/10.1016/j.nlm.2019.01.004>
- Limperopoulos, C., Chilingaryan, G., Guizard, N., Robertson, R. L., & Du Plessis, A. J. (2010). Cerebellar injury in the premature infant is associated with impaired

- growth of specific cerebral regions. *Pediatric Research*, 68(2), 145–150.
<https://doi.org/10.1203/PDR.0b013e3181e1d032>
- Lin, C. Y., Chen, C. H., Tom, S. E., & Kuo, S. H. (2020). Cerebellar Volume Is Associated with Cognitive Decline in Mild Cognitive Impairment: Results from ADNI. *Cerebellum*, 1. <https://doi.org/10.1007/s12311-019-01099-1>
- Margulies, D. S., Ghosh, S. S., Goulas, A., Falkiewicz, M., Huntenburg, J. M., Langs, G., ... Smallwood, J. (2016). Situating the default-mode network along a principal gradient of macroscale cortical. *Proceedings of the National Academy of Sciences*, 113(44), 12574–12579. <https://doi.org/10.1073/pnas.1608282113>
- Matura, S., Prvulovic, D., Jurcoane, A., Hartmann, D., Miller, J., Scheibe, M., ... Pantel, J. (2014). Differential effects of the ApoE4 genotype on brain structure and function. *NeuroImage*, 89, 81–91.
<https://doi.org/10.1016/j.neuroimage.2013.11.042>
- Möller, C., Vrenken, H., Jiskoot, L., Versteeg, A., Barkhof, F., Scheltens, P., & van der Flier, W. M. (2013). Different patterns of gray matter atrophy in early- and late-onset Alzheimer's disease. *Neurobiology of Aging*, 34(8), 2014–2022.
<https://doi.org/http://dx.doi.org/10.1016/j.neurobiolaging.2013.02.013>
- Oh, H., Madison, C., Villeneuve, S., Markley, C., & Jagust, W. J. (2014). Association of gray matter atrophy with age, β -amyloid, and cognition in aging. *Cerebral Cortex*, 24(6), 1609–1618. <https://doi.org/10.1093/cercor/bht017>
- Ramanoël, S., Hoyau, E., Kauffmann, L., Renard, F., Pichat, C., Boudiaf, N., ... Baciù, M. (2018). Gray matter volume and cognitive performance during normal aging A voxel-based morphometry study. *Frontiers in Aging Neuroscience*, 10(AUG), 1–10. <https://doi.org/10.3389/fnagi.2018.00235>
- Raz, N., & Rodrigue, K. M. (2006). Differential aging of the brain: Patterns, cognitive correlates and modifiers. *Neuroscience and Biobehavioral Reviews*, 30(6), 730–748. <https://doi.org/10.1016/j.neubiorev.2006.07.001>
- Rodríguez-Aranda, C., Waterloo, K., Johnsen, S. H., Eldevik, P., Sparr, S., Wikran, G. C., ... Vangberg, T. R. (2016). Neuroanatomical correlates of verbal fluency in early Alzheimer's disease and normal aging. *Brain and Language*, 155–156, 24–35. <https://doi.org/10.1016/j.bandl.2016.03.001>
- Ruscheweyh, R., Deppe, M., Lohmann, H., Wersching, H., Korsukewitz, C., Duning, T., ... Knecht, S. (2013). Executive performance is related to regional gray matter volume in healthy older individuals. *Human Brain Mapping*, 34(12), 3333–3346. <https://doi.org/10.1002/hbm.22146>
- Schmahmann, J. D. (2000). The role of the cerebellum in affect and psychosis. *Journal of Neurolinguistics*, 13(2–3), 189–214. [https://doi.org/10.1016/S0911-6044\(00\)00011-7](https://doi.org/10.1016/S0911-6044(00)00011-7)
- Schmahmann, J. D. (2004). Disorders of the Cerebellum: Ataxia, Dysmetria of Thought, and the Cerebellar Cognitive Affective Syndrome. *The Journal of Neuropsychiatry and Clinical Neurosciences*, 16(3), 367–378.
<https://doi.org/10.1176/jnp.16.3.367>
- Schmahmann, J. D., Guell, X., Stoodley, C. J., & Halko, M. A. (2019). The Theory and Neuroscience of Cerebellar Cognition. *Annual Review of Neuroscience*, 42(1), 337–364. <https://doi.org/10.1146/annurev-neuro-070918-050258>
- Serra, L., Bruschini, M., Di Domenico, C., Gabrielli, G. B., Marra, C., Caltagirone, C., ... Bozzali, M. (2017). Memory is not enough: The neurobiological substrates of dynamic cognitive reserve. *Journal of Alzheimer's Disease*, 58(1), 171–184. <https://doi.org/10.3233/JAD-170086>
- Sullivan, E. V., & Pfefferbaum, A. (2006). Diffusion tensor imaging and aging.

- Neuroscience and Biobehavioral Reviews*, 30(6), 749–761.
<https://doi.org/10.1016/j.neubiorev.2006.06.002>
- Tabatabaei-Jafari, H., Walsh, E., Shaw, M. E., & Cherbuin, N. (2017). The cerebellum shrinks faster than normal ageing in Alzheimer’s disease but not in mild cognitive impairment. *Human Brain Mapping*, 38(6), 3141–3150.
<https://doi.org/10.1002/hbm.23580>
- Thomann, P. A., Schläfer, C., Seidl, U., Santos, V. Dos, Essig, M., & Schröder, J. (2008). The cerebellum in mild cognitive impairment and Alzheimer’s disease - A structural MRI study. *Journal of Psychiatric Research*, 42(14), 1198–1202.
<https://doi.org/10.1016/j.jpsychires.2007.12.002>
- Toniolo, S., Serra, L., Olivito, G., Marra, C., Bozzali, M., & Cercignani, M. (2018). Patterns of cerebellar gray matter atrophy across Alzheimer’s disease progression. *Frontiers in Cellular Neuroscience*, 12(November), 1–8.
<https://doi.org/10.3389/fncel.2018.00430>
- Turkeltaub, P. E., Eden, G. F., Jones, K. M., & Zeffiro, T. A. (2002). Meta-analysis of the functional neuroanatomy of single-word reading: method and validation. *NeuroImage*, 16(3 Pt 1), 765–780. Retrieved from
<http://www.ncbi.nlm.nih.gov/pubmed/12169260>
- Uwisengyimana, J. de D., Nguchu, B. A., Wang, Y., Zhang, D., Liu, Y., Qiu, B., & Wang, X. (2020). Cognitive function and cerebellar morphometric changes relate to abnormal intra-cerebellar and cerebro-cerebellum functional connectivity in old adults. *Experimental Gerontology*, 140(June), 111060.
<https://doi.org/10.1016/j.exger.2020.111060>
- Wickham, H. (2016). *ggplot2: Elegant Graphics for Data Analysis*. Retrieved from
<https://ggplot2.tidyverse.org>
- Zhang, H., Sachdev, P. S., Wen, W., Kochan, N. A., Crawford, J. D., Slavin, M. J., ... Trollor, J. N. (2013). Grey Matter Correlates of Three Language Tests in Non-demented Older Adults. *PloS One*, 8(11), e80215.
<https://doi.org/10.1371/journal.pone.0080215>

Author credits

HMG: conceptualisation, data curation, methodology, software, validation, formal analysis, investigation, visualisation, project administration, writing - original draft, writing – review & editing

XG: conceptualisation, methodology, software, visualisation, writing – review & editing

SS: conceptualisation, methodology, writing – review & editing, supervision

1. We compared cerebellar grey matter loss in Alzheimer’s disease and normal aging.
2. Posterior cerebellum was affected by both healthy aging and Alzheimer’s disease.

3. Healthy aging showed bilateral grey matter loss, while AD was right lateralized.
4. Affected regions participate in default, frontoparietal and attention networks.
5. AD and aging show partly divergent and convergent cerebellar functional profiles.

1. We compared cerebellar grey matter loss in Alzheimer's disease and normal aging.
2. Posterior cerebellum was affected by both healthy aging and Alzheimer's disease.
3. Healthy aging showed bilateral grey matter loss, while AD was right lateralized.
4. Affected regions participate in default, frontoparietal and attention networks.
5. AD and aging show partly divergent and convergent cerebellar functional profiles.

Appendix A – Details of systematic literature search

Table A1. Search terms for the systematic literature search.

Date	Database	Search Terms and Restrictions	N identified studies
Searched			
October 1st 2019	Pubmed	<i>(ag*ing OR elderly OR older adults OR age-related) AND (voxel-based morphometry OR VBM OR grey matter OR gray matter) in Title/Abstract; filter: human</i>	1766
	PsycInfo	<i>(ag*ing OR elderly OR older adults OR age-related) AND (voxel-based morphometry OR VBM OR grey matter OR gray matter) in Abstract (filter: human, peer-reviewed journals, English)</i>	1078
Unique records			2031

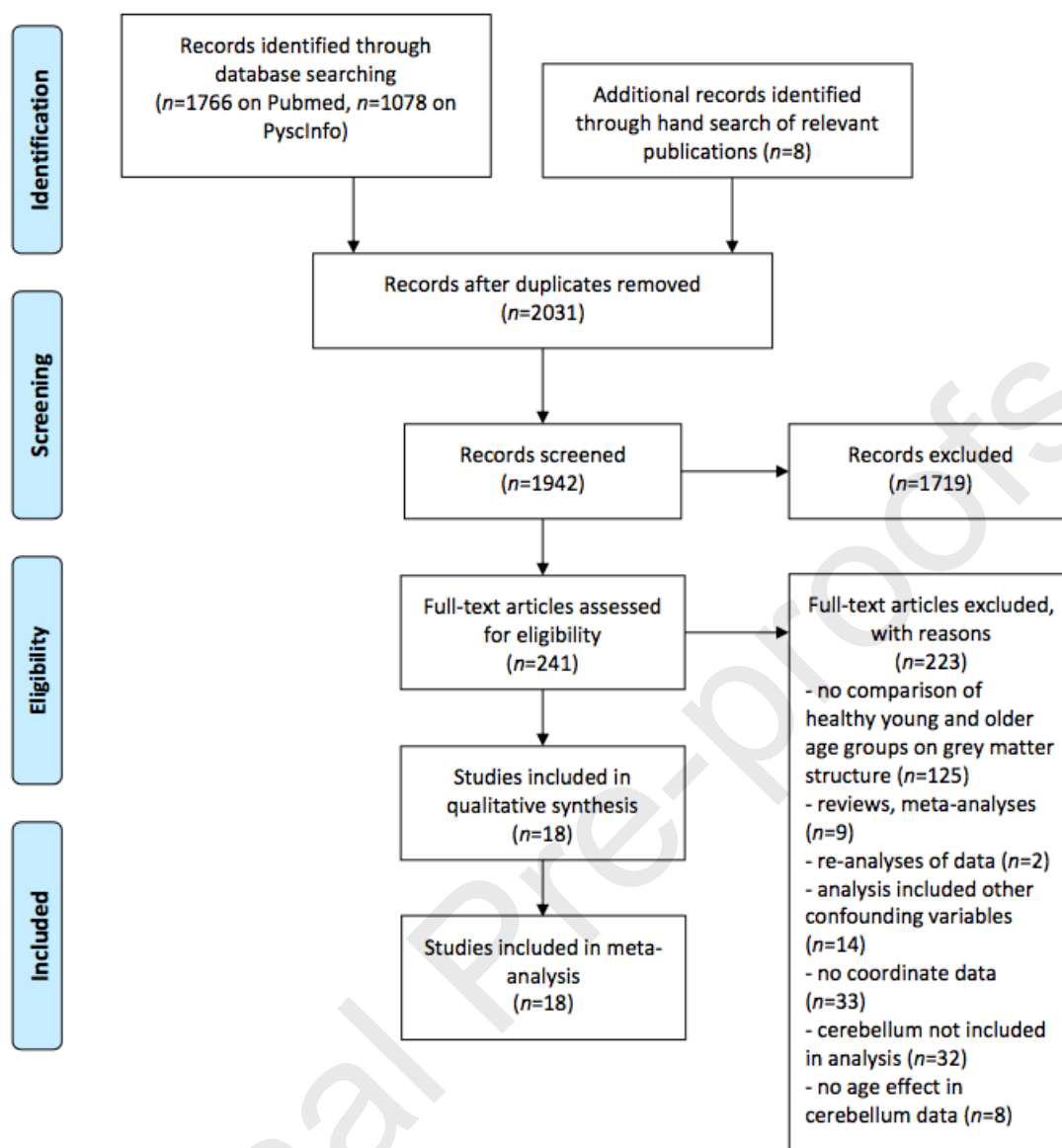


Figure A1. PRISMA flowchart of the study selection procedure.

Appendix B – Study Characteristics

Table B1. Summary of studies included in the meta-analysis of cerebellar grey matter loss in healthy ageing.

<i>Studies using direct comparisons of age groups</i>							
Author, year	N (% female)	Age ± SD (range)	Software	Preprocessing	Nuisance covariates; significance level	Foci for age effect (MNI)	Cognitive vs. young
Maguire & Frith, 2003 [1]	YA 12 (50) OA 12 (50)	YA 32±4 (23-39) OA 75±5 (67-80)	SPM99	Optimised Unmodulated	$p < .05$ corrected	-47 -77 -44	↓ Autobiographical memory retrieval = Memory for autobiographical events = Memory for general knowledge

Steffener, Brickman, Rakitin, Gazes, & Stern, 2009 [2]	YA 37 (22) OA 15 (53)	YA 25±4 OA 75±7	SPM5	Optimised Modulated	Normalised whole brain volume $p < .005$ uncorrected	6 -74 -12	↑ Reaction set sizes in working memory
Antonova et al., 2009 [3]	YA 10 OA 10	YA 24±2 (20-26) OA 72±5 (64-79)	SPM2	Optimised Modulated	NA $p < .05$ FWE	-22 -58 -32 3 -75 -17 39 -69 -25 27 -57 -29 26 -48 -30 ^a	↓ Accuracy location of spatial scene
Bauer, Gebhardt, Gruppe, Gallhofer, & Sammer, 2012 [4]	YA 18 OA 18	YA 24±2 (19-28) OA 60±6 (54-77)	SPM8	Unified DARTEL Modulated	TIV $p < .05$ FWE	30 -66 -30 -23 -75 -23	↑ Reaction location p = Errors in task
Kalpouzos, Persson, & Nyberg, 2012 [5]	YA 16 (50) OA 20 (100)	YA 25 (21-39) OA 61 (52-69)	SPM5	Unified Modulated	$p < .001$ FEW	-26 -35 -38	Unclear
Author, year	N (% female)	Age ± SD (range)	Software	Preprocessing	Nuisance covariates; significance level	Foci for age effect (MNI)	Cognitive vs. young
Bauer, Sammer, & Toepfer, 2018) [6]	YA 35 (57) OA 35 (49)	YA 27±5 (20-35) ^b OA 61±7 (50-80) ^b	SPM12	Pipeline through CAT12 Modulated	TIV, gender, years of education $p < .05$ FWE	29 -77 -39 -32 -72 -41 -24 -45 -41 -45 -53 -45	↑ Errors in working memory Block-Tap
<i>Studies using age as continuous variable</i>							
Good et al., 2001 [7]	465 (43)	30 ^c (17-79)	SPM99	Optimised Modulated	TIV, linear and nonlinear age effects $p < .05$ corrected for multiple comparisons	31 -90 -34	NA
Alexander et al., 2006 [8]	26 (42)	51±16 (22-77)	SPM2	Optimised Modulated	TIV $z \geq -2$	38 -89 -26 ^a	No cognitive (MMSE > 20) participation
Abe et al., 2008 [9]	73 (100)	39.2±14.9 (22-70)	SPM2	Optimised Modulated	TIV $p < .05$ FWE	26 -86 -32 -24 -88 -32	NA
Kalpouzos et al., 2009 [10]	45 (53)	49±18 (20-83)	SPM2	Optimised Modulated	$p < .01$ FDR minimum cluster size $k=20$	-46 -46 -41 36 -43 -44	NA
Bergfield et al., 2010 [11]	29 ^d (62)	48±19 (23-84)	SPM2	Optimised Modulated	TIV $z \geq -2$	52 -47 -29 ^a	NA

Author, year	<i>N</i> (% female)	Age ± <i>SD</i> (range)	Software	Preprocessing	Nuisance covariates; significance level	Foci for age effect (MNI)	Cognitive vs. young
Draganski et al., 2011 [12]	26 (27)	52 (18-85)	SPM8	Unified, DARTEL Modulated	Gender, TIV <i>p</i> <.05 FWE	-36 -58 -31 39 -58 -32	NA
Salami, Eriksson, & Nyberg, 2012 [13]	292 (52)	60±13 (25-80)	SPM8	Unified DARTEL	Age and square of orthogonalised age TIV <i>p</i> <.05 FDR	35 -60 -30	↓ Names face-name
Ziegler et al., 2012 [14]	547 (56)	48±17	SPM8	Optimised Modulated	Scanning site, linear and quadratic age effects <i>p</i> <.05 FWE	15 -54 -17 20 -61 -57 -20 -55 -18 -20 -79 -35 6 -72 -44	NA
Thürling et al., 2014) [15]	34 (56)	42±16 (21-74)	SPM8	SUIT normalised Modulated	TIV <i>p</i> <.05 FWE	-8 -67 -23 18 -74 -29 -13 -48 -43 -30 -61 -20 -35 -70 -41 -4 -75 -20 35 -73 -39 -30 -85 -25 49 -64 -27 -30 -52 -18 32 -65 -18 -13 -66 -42 -41 -76 -39 -35 -61 -50 8 -67 -25 -41 -73 -29 36 -65 -25 -11 -73 -39 49 -55 -29	↓ Storage visual thro responses total cereb
Author, year	<i>N</i> (% female)	Age ± <i>SD</i> (range)	Software	Preprocessing	Nuisance covariates; significance level	Foci for age effect (MNI)	Cognitive vs. young
Dickie et al., 2015 [16]	80 (50)	43 ^e (25-64)	FSL- VBM	Optimised Modulated	NA <i>p</i> <.05 FDR	20 -66 -28 -48 -60 -30	NA
Yu, Korgaonkar, & Grieve, 2017 [17]	438 ^f (58)	32±19 (7-86)	SPM8	SUIT normalised Modulated	TIV, gender, scanning site <i>p</i> <.05 FWE	-37 -39 -39 51 -55 -31 -3 -80 -28 -31 -82 -38 34 -83 -38 -7 -65 -44 17 -31 -21 2 -67 -14 10 -66 -41 -35 -82 -39	NA
Hu et al., 2018	149	32±12	SPM8	DARTEL	NA	-35 -82 -39	↑ Reactio

[18]	(56)	(18-72)	Modulated	$p < .05$ FWE	-8 -70 -14 -39 -40 -42 38 -40 -42 38 -79 -39	signal task
------	------	---------	-----------	---------------	-------------------------------------------------------	-------------

^aCoordinates transformed from Talairach & Tournoux to MNI

^bNumbers based on mean of high and low performing cognitive group

^cMean of four medians from four groups of participants (right-handed females, right-handed males, left-handed females, left-handed males)

^dOnly data from Group 1 included because Group 2 was assessed in Alexander et al. (2006)

^eMedian age

^fTotal study sample size minus 41 subjects who were excluded from the VBM analysis

Abbreviations. CAT: computational anatomy toolbox. DARTEL: diffeomorphic anatomical registration through exponentiated lie algebra; FDR: false discovery rate. FWE: familywise error; FSL: functional magnetic imaging of the brain (FMRIB) software library; GM: grey matter. MA: middle-aged adults. MNI: Montreal Neurological Institute; N: sample size; NA: not applicable; OA: older adults. ROI: region of interest. SD: Standard Deviation. SPM: Statistical Parametric Mapping. SUIT: spatially unbiased infratentorial template. TIV: total intracranial volume. VBM: voxel-based morphometry. YA: younger adults.

Table B2. Study characteristics of records included in the coordinate-based meta-analysis.

Studies are listed according to the degree of cognitive impairment going from least to most severe as measured using the MMSE. Note that this table is based on Gellersen et al. (2017)*:

<https://jnp.bmj.com/content/88/9/780.full#DC1>.

Authors	Notes on diagnosis	<i>N</i> patients (% female)	<i>N</i> controls (% female)	Age patients ± <i>SD</i>	Age controls ± <i>SD</i>	<i>p</i> -value age difference	MMSE or ACE patients ± <i>SD</i>	Disease Duration (years ± <i>SD</i>)	Coordinates (MNI)
Farrow et al., 2007 [19]	Probable AD based on NINCDS-ADRDA criteria	7	11	78±7	71±4	.014	25±4 (MMSE)	4	25 -40 -29 -24 -36 -29
Mazère et al., 2008 [20]	Probable based on NINCDS-ADRDA criteria	8 (63)	8 (75)	80±7	74±3	NS	24±2 (MMSE)	NA	-44 -65 -42 27 -66 -11
Ossenkoppele et al., 2015 [21]	Subgroup of AD patients defined as typical AD based on NIA-AA criteria; biomarker confirmed	58 (39)	61 (38)	64±9	64±8	NS	23±4 (MMSE)	NA	-39 -82 -33 46 -73 -36
Canu et al., 2011 [22]	Based on NINCDS- ADRDA criteria	17 (82)	13 (46)	77±6	73±7	NS	21±5 (MMSE)	NA	42 -59 -25 32 -64 -36 -29 -70 -39 -36 -67 -32
Möller et al., 2013 [23]	Subgroup of late- onset probable AD based on NINCDS- ADRDA criteria	120 (46)	71 (50)	72±5	71±4	NS	21±5 (MMSE)	NA	33 -60 -27 30 -69 -38 12 -61 -23 26 -49 -47 -26 -48 -45 -34 -48 -45 -30 -42 -42 10 -67 -36
Colloby, O'Brien, & Taylor, 2014 [24]	Probable AD based on NINCDS-ADRDA criteria	47	39	79±9	77±6	NS	21±4 (MMSE)	NA	-33 -43 -24 42 -43 -26
Authors	Notes on diagnosis	<i>N</i> patients (% female)	<i>N</i> controls (% female)	Age patients ± <i>SD</i>	Age controls ± <i>SD</i>	<i>p</i> -value age difference	MMSE or ACE patients ± <i>SD</i>	Disease Duration (years ± <i>SD</i>)	Coordinates (MNI)
Canu et al., 2012 [25]	Subgroup of late- onset probable AD based on NINCDS- ADRDA criteria	24 (67)	24 (71)	78±5	76±4	NS	21±4 (MMSE)	4±2	33 -75 -28
Toniolo et al., 2018 [26]	Probable AD based on NINCDS-ADRDA criteria	53 (66)	34 (50)	75±6	69±7	NS	20±3 (MMSE)	NA	19 -35 -19 39 -63 -23 -4 -51 -26

Lehmann et al., 2011 [27]	Probable AD based on NINCDS-ADRDA criteria; typical AD presentation.	30 (53)	50 (66)	69±9	63±10	<.005	19±5 (MMSE)	5	8 -49 -30
Serra et al., 2014 [28]	Probable AD based on NINCDS-ADRDA criteria	48 (35)	20 (65)	71±6	70±6	NS	19±3 (MMSE)	4±3	-12 -86 -24

Authors	Notes on diagnosis	<i>N</i> patients (% female)	<i>N</i> controls (% female)	Age patients ± <i>SD</i>	Age controls ± <i>SD</i>	<i>p</i> -value age difference	MMSE or ACE patients ± <i>SD</i>	Disease Duration (years ± <i>SD</i>)	Coordinates (MNI)
Guo et al., 2016 [29]	Probable AD based on NINCDS-ADRDA criteria	34 (44)	34 (53)	62±6	64±5	NS	NA (MMSE)	3±3	-32 -72 -29 -31 -60 -19 27 -71 -28 27 -76 -26
Raji et al., 2009 [30]	Probable AD based on NINCDS-ADRDA criteria	33 (33)	169 (57)	83±5	78±4	.001	76±13 ^a (MMSE)	NA	-24 -33 -31 28 -33 -34 1 -37 -20
Ahmed et al., 2019 [31]	Probable AD based on NINCDS-ADRDA criteria	16 (38)	19 (32)	60±6	63±7	NS	62±16 (ACE-III)	4±2	-52 -58 -46 42 -52 -58

^aUse of modified MMSE.

Abbreviations. ACE-III: Addenbrookes Cognitive Examination – Version 3. AD: Alzheimer’s disease. ADAS-TES: Alzheimer’s Disease Assessment Scale Total Error Score. CAMCOG: Cambridge Cognitive Examination. MMSE: Mini Mental State Exam. MNI: Montreal Neurological Institute. NA: not available. NIA-AA: National Institute on Aging-Alzheimer’s Association. NINCDS-ADRDA: National Institute of Neurological and Communicative Disorders and Stroke and Alzheimer’s Disease and Related Disorders Association. NS: not significant. RAVLT: Rey Auditory Verbal Learning Test. RCFT: Rey Complex Figure Test. SD: Standard Deviation.

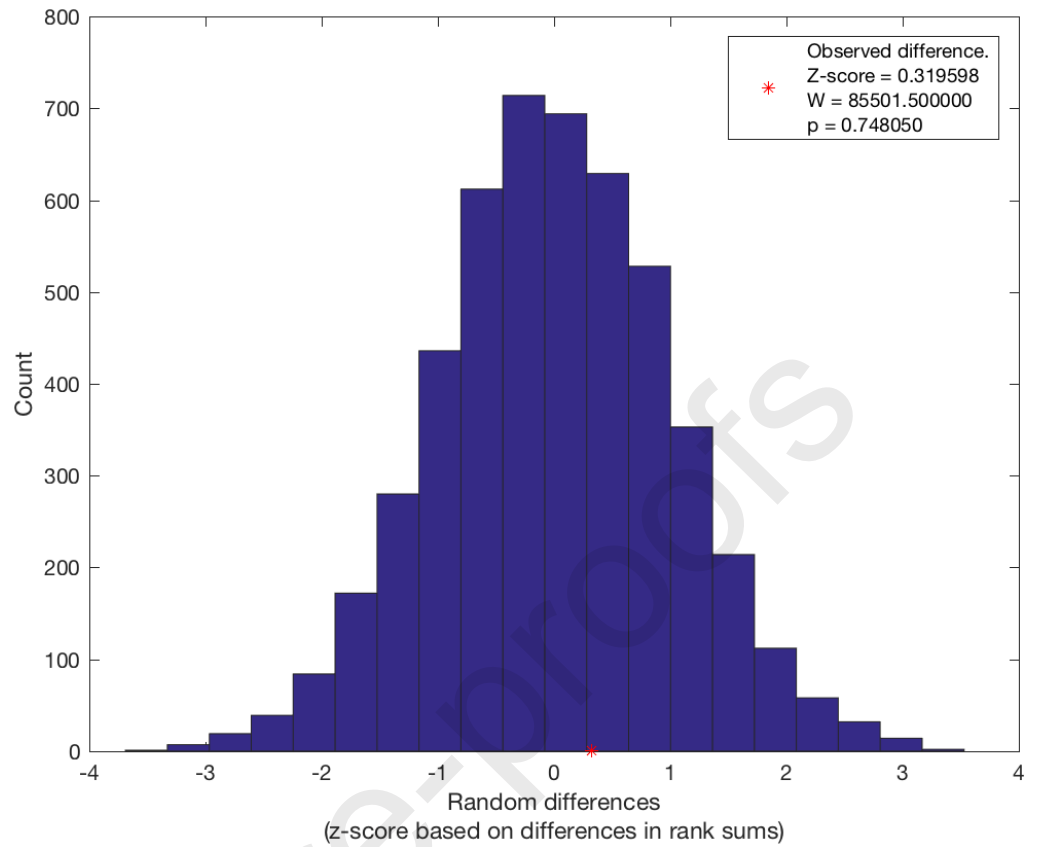
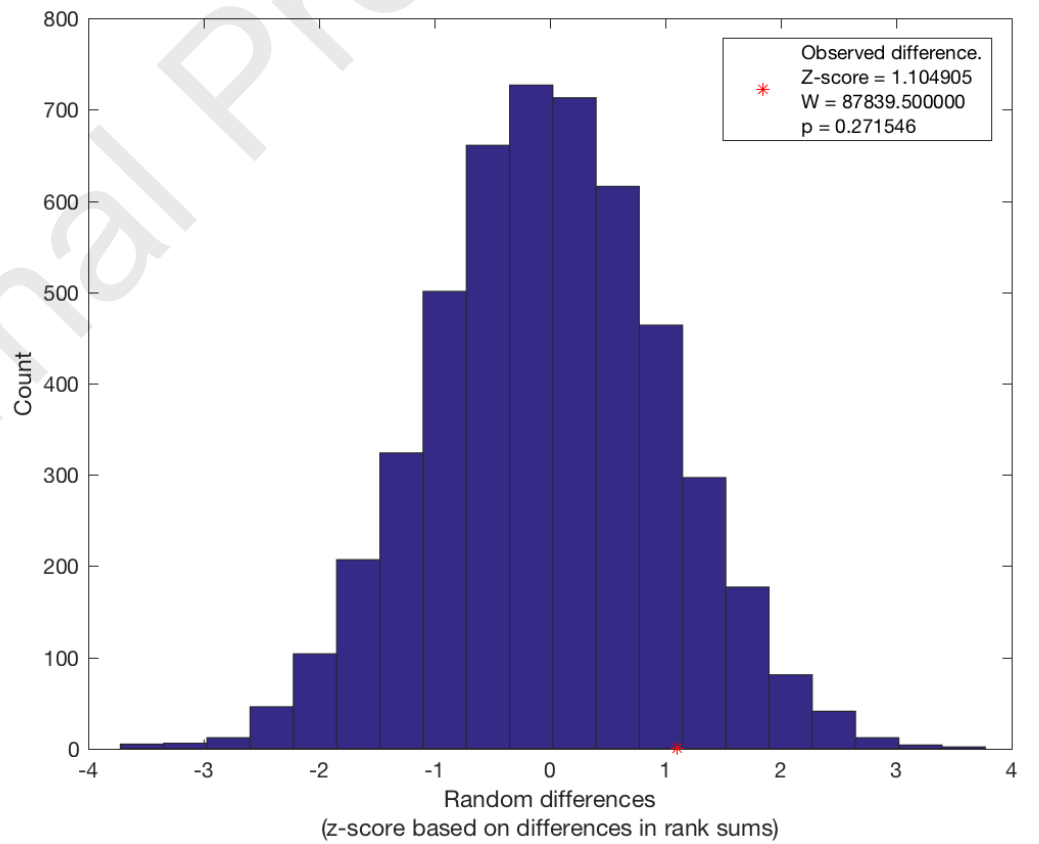
References

- [1] Maguire EA, Frith CD. Aging affects the engagement of the hippocampus during autobiographical memory retrieval. *Brain* 2003;126:1511–23. doi:10.1093/brain/awg157.
- [2] Steffener J, Brickman AM, Rakitin BC, Gazes Y, Stern Y. The impact of age-related changes on working memory functional activity. *Brain Imaging Behav* 2009;3:142–53. doi:10.1007/s11682-008-9056-x.
- [3] Antonova E, Parslow D, Brammer M, Dawson GR, Jackson SHDD, Morris RG. Age-related neural activity during allocentric spatial memory. *Memory* 2009;17:125–43. doi:10.1080/09658210802077348.
- [4] Bauer E, Gebhardt H, Gruppe H, Gallhofer B, Sammer G. Altered negative priming in older subjects: First evidence from behavioral and neural level. *Front Hum Neurosci* 2012;6:1–10. doi:10.3389/fnhum.2012.00270.
- [5] Kalpouzos G, Persson J, Nyberg L. Local brain atrophy accounts for functional activity differences in normal aging. *Neurobiol Aging* 2012;33:e1–13. doi:10.1016/j.neurobiolaging.2011.02.021.
- [6] Bauer E, Sammer G, Toepper M. Performance level and cortical atrophy modulate the neural response to increasing working memory load in younger and older adults. *Front Aging Neurosci* 2018;10:1–15. doi:10.3389/fnagi.2018.00265.
- [7] Good CD, Johnsrude IS, Ashburner J, Henson RNA, Friston KJ, Frackowiak RSJ. A voxel-based morphometric study of ageing in 465 normal adult human brains. *Neuroimage* 2001;14:21–36. doi:10.1006/nimg.2001.0786.
- [8] Alexander GE, Chen K, Merkle TL, Reiman EM, Caselli RJ, Aschenbrenner M, et al. Regional network of magnetic resonance imaging gray matter volume in healthy aging. *Neuroreport* 2006;17:951–6. doi:10.1097/01.wnr.0000220135.16844.b6.
- [9] Abe O, Yamasue H, Aoki S, Suga M, Yamada H, Kasai K, et al. Aging in the CNS: comparison of gray/white matter volume and diffusion tensor data. *Neurobiol Aging* 2008;29:102–16. doi:10.1016/j.neurobiolaging.2006.09.003.
- [10] Kalpouzos G, Chételat G, Baron JC, Landeau B, Mevel K, Godeau C, et al. Voxel-based mapping of brain gray matter volume and glucose metabolism profiles in normal aging. *Neurobiol Aging* 2009;30:112–24. doi:10.1016/j.neurobiolaging.2007.05.019.
- [11] Bergfield KL, Hanson KD, Chen K, Teipel SJ, Hampel H, Rapoport SI, et al. Age-related networks of regional covariance in MRI gray matter: Reproducible multivariate patterns in healthy aging. *Neuroimage* 2010;49:1750–9. doi:10.1016/j.neuroimage.2009.09.051.
- [12] Draganski B, Ashburner J, Hutton C, Kherif F, Frackowiak RSJJ, Helms G, et al. Regional specificity of MRI contrast parameter changes in normal ageing revealed by voxel-based quantification (VBQ). *Neuroimage* 2011;55:1423–34. doi:10.1016/j.neuroimage.2011.01.052.
- [13] Salami A, Eriksson J, Nyberg L. Opposing effects of aging on large-scale Brain systems for memory encoding and cognitive control. *J Neurosci* 2012;32:10749–57. doi:10.1523/JNEUROSCI.0278-12.2012.
- [14] Ziegler G, Dahnke R, Jäncke L, Yotter RA, May A, Gaser C. Brain structural trajectories over the adult lifespan. *Hum Brain Mapp* 2012;33:2377–89. doi:10.1002/hbm.21374.
- [15] Thürling M, Galuba J, Thieme A, Burciu RG, Goricke S, Beck A, et al. Age effects in storage and extinction of a naturally acquired conditioned eyeblink response. *Neurobiol Learn Mem* 2014;109:104–12. doi:10.1016/j.nlm.2013.12.007.
- [16] Dickie DA, Mikhael S, Job DE, Wardlaw JM, Laidlaw DH, Bastin ME. Permutation and parametric tests for effect sizes in voxel-based morphometry of gray matter volume in brain structural MRI. *Magn Reson Imaging* 2015;33:1299–305. doi:10.1016/j.mri.2015.07.014.
- [17] Yu T, Korgaonkar MS, Grieve SM. Gray matter atrophy in the cerebellum—Evidence of increased vulnerability of the crus and vermis with advancing age. *The Cerebellum* 2017;16:388–97. doi:10.1007/s12311-016-0813-x.
- [18] Hu S, Ide JS, Chao HH, Castagna B, Fischer KA, Zhang S, et al. Structural and functional cerebral bases of diminished inhibitory control during healthy aging. *Hum Brain Mapp* 2018;39:5085–5096. doi:10.1002/hbm.24347.
- [19] Farrow TFD, Thiyagesh SN, Wilkinson ID, Parks RW, Ingram L, Woodruff PWR. Fronto-temporal-lobe atrophy in early-stage Alzheimer’s disease identified using an improved detection methodology. *Psychiatry Res* 2007;155:11–9. doi:10.1016/j.psychres.2006.12.013.
- [20] Mazère J, Prunier C, Barret O, Guyot M, Hommet C, Guilloteau D, et al. In vivo SPECT imaging of vesicular acetylcholine transporter using [123I]-IBVM in early Alzheimer’s disease. *Neuroimage* 2008;40:280–8. doi:10.1016/j.neuroimage.2007.11.028.

- [21] Ossenkoppele R, Pijnenburg YAL, Perry DC, Cohn-Sheehy BI, Scheltens NME, Vogel JW, et al. The behavioural/dysexecutive variant of Alzheimer's disease: Clinical, neuroimaging and pathological features. *Brain* 2015;138:2732–49. doi:10.1093/brain/awv191.
- [22] Canu E, McLaren DG, Fitzgerald ME, Bendlin BB, Zoccatelli G, Alessandrini F, et al. Mapping the structural brain changes in Alzheimer's disease: The independent contribution of two imaging modalities. *Adv Alzheimer's Dis* 2011;2:487–98. doi:10.3233/978-1-60750-793-2-487.
- [23] Möller C, Vrenken H, Jiskoot L, Versteeg A, Barkhof F, Scheltens P, et al. Different patterns of gray matter atrophy in early- and late-onset Alzheimer's disease. *Neurobiol Aging* 2013;34:2014–22. doi:http://dx.doi.org/10.1016/j.neurobiolaging.2013.02.013.
- [24] Colloby SJ, O'Brien JT, Taylor JP. Patterns of cerebellar volume loss in dementia with Lewy bodies and Alzheimer's disease: A VBM-DARTEL study. *Psychiatry Res - Neuroimaging* 2014;223:187–91. doi:10.1016/j.psychres.2014.06.006.
- [25] Canu E, Frisoni GB, Agosta F, Pievani M, Bonetti M, Filippi M. Early and late onset Alzheimer's disease patients have distinct patterns of white matter damage. *Neurobiol Aging* 2012;33:1023–33. doi:10.1016/j.neurobiolaging.2010.09.021.
- [26] Toniolo S, Serra L, Olivito G, Marra C, Bozzali M, Cercignani M. Patterns of cerebellar gray matter atrophy across Alzheimer's disease progression. *Front Cell Neurosci* 2018;12:1–8. doi:10.3389/fncel.2018.00430.
- [27] Lehmann M, Crutch SJ, Ridgway GR, Ridha BH, Barnes J, Warrington EK, et al. Cortical thickness and voxel-based morphometry in posterior cortical atrophy and typical Alzheimer's disease. *Neurobiol Aging* 2011;32:1466–76. doi:10.1016/j.neurobiolaging.2009.08.017.
- [28] Serra L, Fadda L, Perri R, Spanò B, Marra C, Castelli D, et al. Constructional apraxia as a distinctive cognitive and structural brain feature of pre-senile Alzheimer's disease. *J Alzheimer's Dis* 2014;38:391–402. doi:10.3233/JAD-130656.
- [29] Guo CC, Tan R, Hodges JR, Hu X, Sami S, Hornberger M. Network-selective vulnerability of the human cerebellum to Alzheimer's disease and frontotemporal dementia. *Brain* 2016;139:1527–38. doi:10.1093/brain/aww003.
- [30] Raji CA, Lopez OL, Kuller LH, Carmichael OT, Becker JT. Age, Alzheimer disease, and brain structure. *Neurology* 2009;73:1899–905. doi:10.1212/WNL.0b013e3181c3f293.
- [31] Ahmed RM, Landin-Romero R, Liang CT, Keogh JM, Henning E, Strikwerda-Brown C, et al. Neural networks associated with body composition in frontotemporal dementia. *Ann Clin Transl Neurol* 2019;6:1707–17. doi:10.1002/acn3.50869.

Appendix C – Testing Gradient Differences in Ageing and Alzheimer's Disease

a.

**b.**

c.

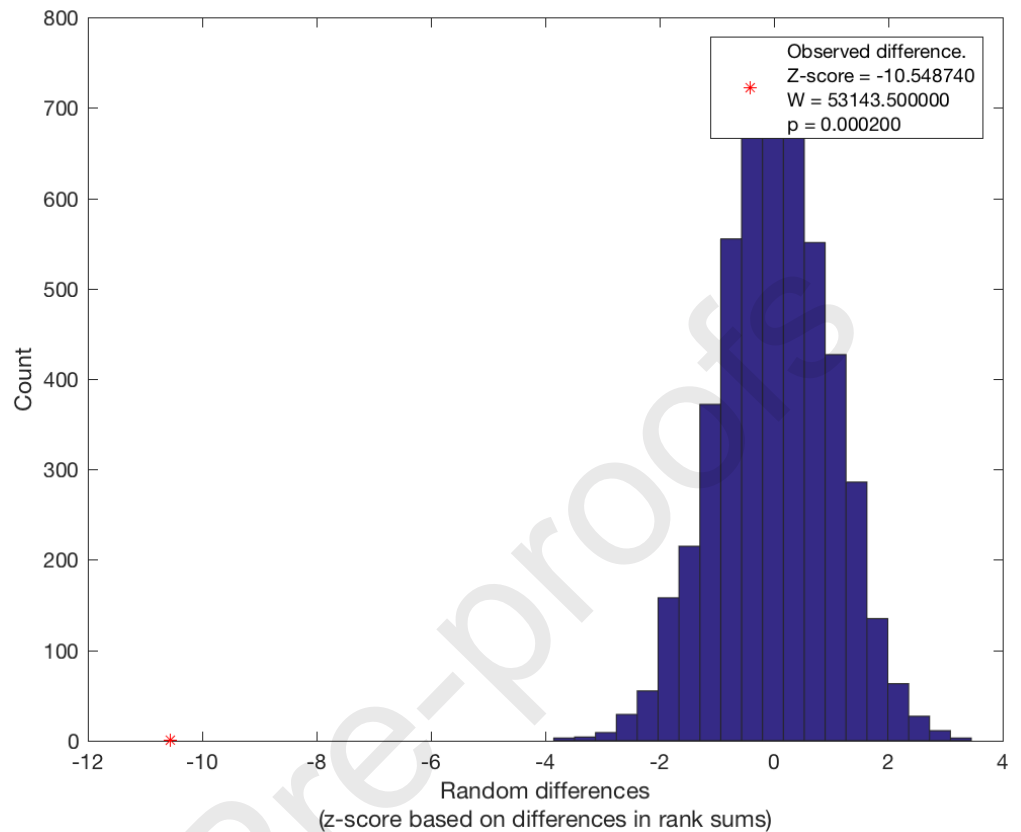


Figure C1. Results of the permutation analysis to assess differences in values of the functional gradients for AD- and age-related grey matter decline. Observed differences between healthy ageing and AD gradient values were computed using a Wilcoxon rank sum test and a subsequent conversion of ranks to z-scores. Positive differences indicate higher values for the healthy ageing compared to the AD group. Observed differences are marked with a red asterisk. Random differences were calculated based on random allocation of a given gradient value to the ageing or AD group. a. Gradient 1 values. B. Gradient 2 values. c. Gradient 3 values.

Appendix D – Results of Robustness Tests

Results of each jackknife analysis can be found in Table D1. A count of the occurrences of cluster survival, size changes, and peak location shifts revealed that, for the case of healthy ageing, there was no case in which a one study removed analysis changed the label of the peak voxel of a cluster (Table D2). Only slight shifts in peak voxel locations were observed. The jackknife procedure showed that clusters 1 and 2 in right Crus I/II were robust to the removal of any one study. Only

unsubstantial changes in size and extent of these clusters occurred. Cluster 3 in posterior Crus II did not survive the removal of the study by Hu et al. [1] ($n=149$ subjects, $k=5$ foci), while cluster 4 in vermal/right lobule VI did no longer emerge when the study by Antonova et al. [2] ($n=20$, $k=5$ foci) was removed. Both cluster 3 and 4 remained stable in all other instances, indicating robustness in 94% of analyses. Finally, cluster 5 in anterior Crus I/II remained in 83% of all analyses but did not survive correction for multiple comparisons upon removal of studies that were the main contributors to this cluster [1–4]. These also tended to be studies with a larger number of foci.

The two clusters for the AD meta-analysis remained present 85% of all jackknife analyses (Table D2), with two studies each resulting in either cluster 1 or cluster 2 not surviving the FEW $p<.05$ threshold (but it was never the case that both clusters disappeared).

In five instances, the two clusters merged into one larger cluster. Changes in the coordinate of the peak location of the cluster did occur but this change never affected the label of this location. In five cases, the cluster size was reduced (removal of studies by [5–9]).

Figures D1-3 show cerebellar flatmaps and gradient maps for all one-study-removed analyses to visualise the changes in structural age and AD effects and their localisation onto functional gradients caused by the removal of each individual study. We further assessed the effect of the jackknifing procedure on mean gradient values and tested whether the difference in gradient values we observed between our full ageing analysis with all studies included and our previous AD meta-analysis was robust to jackknifing (Figure D4 for a distribution of mean gradient values). Running the permutations to test for a difference in gradient values for each of the 13 AD and

18 ageing jackknife analyses revealed that on average, there was no difference in Gradient 1 values between healthy ageing and AD cases (*Mean z-score based on Wilcoxon rank sum* = .145, 95% *CI* [-.682, .973]; *Cohen's U_I* = .215, 95% *CI* [.182, .248]). Likewise, there was no difference in Gradient 2 values (*Mean z* = .928, 95% *CI* [.148, 1.707]; *Cohen's U_I* = .104, 95% *CI* [.071, .137]). The distributions of Gradient 3 values in AD and healthy ageing were significantly non-overlapping across one-study removed analyses (*Mean z* = -9.681, 95% *CI* [-10.381, -8.981]; *Cohen's U_I* = .337, 95% *CI* [.308, .367]).

Table D1. Results of the jackknifing procedure. One study at a time was excluded to test robustness of the clusters from the main analysis.

Study Removed	Number of foci	Number of subjects	Min cluster size (mm ³) by ALE algorithm	Cluster number (by size; ordered according to correspondence to main analysis cluster) ^a	Change in cluster size?	Change in peak coordinate by >2 in any direction?	Change in label of peak coordinates?	Extent (mm ³)	Cluster coordinates
<i>Healthy ageing</i>									
None	64	2441	520	1	NA	NA	NA	1504	(24 -90 -42) to (40 -72 -30) centered at (33 -81 -37)
				2				1464	(28 -70 -34) to (42 -56 -22) centered at (35 -63 -29)
				3				1288	(-46 -86 -44) to (-28 -68 -34) centered at (-35 -77 -40)
				4				1112	(-10 -78 -22) to (8 -66 -10) centered at (1 -72 -15)
				5				808	(-48 -54 -46) to (-34 -36 -36) centered at (-40 -42 -41)
Abe et al., 2008 [11]	62	2368	488	3	↓	No	No	1160	(28 -90 -42) to (40 -72 -32) centered at (34 -80 -38)
				1	↑	No	No	1472	(28 -70 -34) to (42 -56 -22) centered at (35 -63 -29)
				2	=	No	No	1288	(-46 -86 -44) to (-28 -68 -34) centered at (-35 -77 -40)
				4	=	No	No	1112	(-10 -78 -22) to (8 -66 -10) centered at (1 -72 -15)
				5	=	No	No	808	(-48 -54 -46) to (-34 -36 -36) centered at (-40 -42 -41)
Alexander et al., 2006 [12]	63	2415	520	1	↓	No	No	1464	24 -90 -42) to (40 -72 -30) centered at (33 -81 -37)
				2	=	No	No	1464	(28 -70 -34) to (42 -56 -22) centered at (35 -63 -29)
				3	=	No	No	1288	(-46 -86 -44) to (-28 -68 -34) centered at (-35 -77 -40)
				4	=	No	No	1112	(-10 -78 -22) to (8 -66 -10) centered at (1 -72 -15)
				5	=	No	No	808	(-48 -54 -46) to (-34 -36 -36) centered at (-40 -42 -41)

Study Removed	Number of foci	Number of subjects	Min cluster size (mm ³) by ALE algorithm	Cluster number (by size; ordered according to correspondence to main analysis cluster) ^a	Change in cluster size?	Change in peak coordinate by >2 in any direction?	Change in label of peak coordinates?	Extent (mm ³)	Cluster coordinates
Antonova et al., 2009 [2]	59	2421	504	1	=	No	No	1504	(24 -90 -42) to (40 -72 -30) centered at (33 -81 -37)
				3	↓	No	No	920	(28 -68 -34) to (42 -56 -24) centered at (35 -62 -29)
				2	↑	Yes	No	1312	(-48 -86 -44) to (-28 -68 -34) centered at (-35 -77 -49)
				5	NA	NA	NA	NA	NA
				4	=	No	No	808	(-48 -54 -46) to (-34 -36 -36) centered at (-40 -42 -41)
Bauer et al., 2012 [13]	62	2405	504	1	=	No	No	1504	(24 -90 -42) to (40 -72 -30) centered at (33 -81 -37)
				4	↓	No	No	1040	(28 -70 -34) to (42 -56 -22) centered at (36 -62 -28)
				2	↓	No	No	1312	(-46 -86 -44) to (-28 -68 -34) centered at (-35 -77 -40)
				3	=	No	No	1112	(-10 -78 -22) to (8 -66 -10) centered at (1 -72 -15)
				5	=	No	No	808	(-48 -54 -46) to (-34 -36 -36) centered at (-40 -42 -41)
Bauer et al., 2018 [14]	60	2371	464	3	↓	No	No	1152	(24 -90 -42) to (40 -72 -30) centered at (33 -82 -37)
				1	↑	No	No	1520	(26 -70 -34) to (42 -56 -22) centered at (35 -63 -29)
				4	↓	Yes	No	736	(-48 -86 -44) to (-28 -74 -34) centered at (-35 -81 -39)
				2	↑	No	No	1176	(-10 -78 -22) to (8 -66 -10) centered at (1 -72 -15)
				5	↓	Yes	No	616	(-46 -46 -44) to (-34 -36 -36) centered at (-39 -40 -41)
				6	↓	Yes	No	472	(46 -58 -34) to (54 -52 -26) centered at (50 -55 -30)
Note that cluster 5 from the original analysis split into two sub-clusters in this analysis									

Study Removed	Number of foci	Number of subjects	Min cluster size (mm ³) by ALE algorithm	Cluster number (by size; ordered according to correspondence to main analysis cluster) ^a	Change in cluster size?	Change in peak coordinate by >2 in any direction?	Change in label of peak coordinates?	Extent (mm ³)	Cluster coordinates
Bergfield et al., 2009 [15]	63	2412	528	1	=	No	No	1504	(24 -90 -42) to (40 -72 -30) centered at (33 -81 -37)
				2	↑	No	No	1472	(28 -70 -34) to (42 -56 -22) centered at (35 -63 -29)
				3	=	No	No	1288	(-46 -86 -44) to (-28 -68 -34) centered at (-35 -77 -40)
				4	=	No	No	1112	(-10 -78 -22) to (8 -66 -10) centered at (1 -72 -15)
				5	=	No	No	808	(-48 -54 -46) to (-34 -36 -36) centered at (-40 -42 -41)
Dickie et al., 2015 [16]	62	2361	512	1	↑	No	No	1512	(24 -90 -42) to (40 -72 -30) centered at (33 -81 -37)
				2	↑	No	No	1496	(28 -70 -34) to (42 -56 -22) centered at (35 -63 -29)
				3	↑	No	No	1336	(-48 -86 -44) to (-28 -68 -34) centered at (-35 -77 -40)
				4	↑	No	No	1176	(-10 -78 -22) to (8 -66 -10) centered at (1 -72 -15)
				5	=	No	No	808	(-48 -54 -46) to (-34 -36 -36) centered at (-40 -42 -41)
Draganski et al., 2011 [17]	62	2415	496	1	=	No	No	1504	(24 -90 -42) to (40 -72 -30) centered at (33 -81 -37)
				4	↓	No	No	1088	(28 -70 -32) to (40 -58 -22) centered at (34 -64 -28)
				2	↑	No	No	1312	(-48 -86 -44) to (-28 -68 -34) centered at (-35 -77 -40)
				3	=	No	No	1112	(-10 -78 -22) to (8 -66 -10) centered at (1 -72 -15)
				5	=	No	No	808	(-48 -54 -46) to (-34 -36 -36) centered at (-40 -42 -41)

Study Removed	Number of foci	Number of subjects	Min cluster size (mm ³) by ALE algorithm	Cluster number (by size; ordered according to correspondence to main analysis cluster) ^a	Change in cluster size?	Change in peak coordinate by >2 in any direction?	Change in label of peak coordinates?	Extent (mm ³)	Cluster coordinates		
Good et al., 2001 [18]	63	1976	512	4	↓	Yes	No	992	(28 -86 -42) to (40 -72 -36) centered at (34 -78 -39)		
				1	↓	No	No	1472	(28 -70 -34) to (35 -63 -29) centered at (36 -60 -30)		
				2	↑	No	No	1312	(-48 -86 -44) to (-28 -68 -34) centered at (-35 -77 -40)		
				3	↓	No	No	1112	(-10 -78,-22) to (8,-66,-10) centered at (1 -72 -15)		
				5	=	No	No	808	(-48 -54 -46) to (-34 -36 -36) centered at (-40 -42 -41)		
Hu et al., 2018 [1]	59	2293	536	2	↓	No	No	1128	(24 -90 -42) to (40 -72 -30) centered at (33 -81 -37)		
				1	↑	No	No	1544	(26 -70 -34) to (42 -56 -22) centered at (35 -63 -29)		
				Cluster 3 from the original analysis does not survive		NA	NA	NA	NA	NA	NA
				3	↓	No	No	840	(-4 -78 -22) to (8 -66 -10) centered at (3 -73 -15)		
Cluster 5 from the original analysis does not survive											
Kalpouzos et al., 2009 [19]	62	2396	520	1	=	No	No	1504	(24 -90 -42) to (40 -72 -30) centered at (33 -81 -37)		
				2	↑	No	No	1472	(28 -70 -34) to (42 -56 -22) centered at (35 -63 -29)		
				3	↑	No	No	1312	(-46 -86 -44) to (-28 -68 -34) centered at (-35 -77 -40)		
				4	=	No	No	1112	(-10 -78 -22) to (8 -66 -10) centered at (1 -72 -15)		
Cluster 5 from the original analysis does not survive					NA	NA	NA	NA	NA		

Study Removed	Number of foci	Number of subjects	Min cluster size (mm ³) by ALE algorithm	Cluster number (by size; ordered according to correspondence to main analysis cluster) ^a	Change in cluster size?	Change in peak coordinate by >2 in any direction?	Change in label of peak coordinates?	Extent (mm ³)	Cluster coordinates
Kalpouzos et al., 2012 [20]	63	2405	520	1	=	No	No	1504	(24 -90 -42) to (40 -72 -30) centered at (33 -81 -37)
				2	↑	No	No	1472	(28 -70 -34) to (42 -56 -22) centered at (35 -63 -29)
				3	↑	No	No	1312	(-48 -86 -44) to (-28 -68 -34) centered at (-35 -77 -40)
				4	=	No	No	1112	(-10 -78 -22) to (8 -66 -10) centered at (1 -72 -15)
				5	↓	No	No	792	(-48 -54 -46) to (-34 -36 -36) centered at (-40 -42 -41)
Maguire et al., 2003 [21]	63	2417	496	1	=	No	No	1504	(24 -90 -42) to (40 -72 -30) centered at (33 -81 -37)
				2	=	No	No	1472	(28 -70 -34) to (42 -56 -22) centered at (35 -63 -29)
				4	=	No	No	1104	(-42 -86 -44) to (-28 -68 -34) centered at (-33 -77 -40)
				3	↓	No	No	1112	(-10 -78 -22) to (8 -66 -10) centered at (1 -72 -15)
				5	=	No	No	808	(-48 -54 -46) to (-34 -36 -36) centered at (-40 -42 -41)
Salami et al., 2012 [22]	63	2149	504	1	=	No	No	1504	(24 -90 -42) to (40 -72 -30) centered at (33 -81 -37)
				5	↓	Yes	No	624	(28 -70 -32) to (40 -62 -22) centered at (35 -66 -27)
				2	↓	No	No	1312	(-46 -86 -44) to (-28 -68 -34) centered at (-35 -77 -40)
				3	=	No	No	1112	(-10 -78,-22) to (8,-66,-10) centered at (1 -72 -15)
				4	=	No	No	808	(-48 -54 -46) to (-34 -36 -36) centered at (-40 -42 -41)

Study Removed	Number of foci	Number of subjects	Min cluster size (mm ³) by ALE algorithm	Cluster number (by size; ordered according to correspondence to main analysis cluster) ^a	Change in cluster size?	Change in peak coordinate by >2 in any direction?	Change in label of peak coordinates?	Extent (mm ³)	Cluster coordinates
Steffener et al., 2009 [23]	63	2389	560	1	=	No	No	1504	(24 -90 -42) to (40 -72 -30) centered at (33 -81 -37)
				2	=	No	No	1472	(28 -70 -34) to (42 -56 -22) centered at (35 -63 -29)
				3	↑	No	No	1312	(-48 -86 -44) to (-28 -68 -34) centered at (-35 -77 -40)
				5	=	No	No	808	(-48 -54 -46) to (-34 -36 -36) centered at (-40 -42 -41)
				4	↓	No	No	672	(-10 -76 -22) to (4 -66 -12) centered at (1 -72 -16)
Thürling et a., 2014 [24]	45	2407	560	1	↓	No	No	1232	(24 -90 -42) to (40 -76 -30) centered at (33 -83 -37)
				2	↓	No	No	848	(26 -68 -34) to (40 -56 -28) centered at (34 -61 -30)
				5	↓	Yes	No	600	(-38 -86 -42) to (-28 -72 -34) centered at (-33 -81 -39)
				4	↓	Yes	No	648	(-2 -78 -18) to (8 -66 -10) centered at (4 -72 -15)
				3	↓	No	No	832	(-48 -54 -46) to (-34 -36 -36) centered at (-40 -42 -41)
Yu et al., 2017 [3]	55	2003	584	4	↓	Yes	No	656	(28 -80 -42) to (40 -72 -36) centered at (34 -76 -39)
				1	↑	No	No	1592	(28 -70 -34) to (42 -56 -22) centered at (35 -63 -29)
				2	↓	No	No	920	(-48 -84 -40) to (-30 -68 -38) centered at (-36 -75 -41)
				3	↓	No	No	776	(-10 -78,-24) to (8,-66,-10) centered at (1 -73 -16)

Study Removed	Number of foci	Number of subjects	Min cluster size (mm ³) by ALE algorithm	Cluster number (by size; ordered according to correspondence to main analysis cluster) ^a	Change in cluster size?	Change in peak coordinate by >2 in any direction?	Change in label of peak coordinates?	Extent (mm ³)	Cluster coordinates
Cluster 5 from main analysis does not survive					NA	NA	NA	NA	NA
Ziegler et al., 2012 [25]	59	1894	488	1	↑	No	No	1544	(24 -90 -42) to (40 -72 -30) centered at (33 -81 -37)
				2	↑	No	No	1544	(26 -70 -34) to (42 -56 -22) centered at (35 -63 -29)
				3	↑	No	No	1352	(-48 -86 -44) to (-28 -68 -34) centered at (-35 -77 -40)
				4	↑	No	No	1328	(-10 -82,-30) to (8,-66,-10) centered at (0 -73 -17)
				5	↑	No	No	824	(-48 -54 -46) to (-34 -36 -36) centered at (-40 -42 -41)
<i>Alzheimer's disease</i>									
None	35	529	440	1	NA	NA	NA	1144	(26 -78 -40) to (34 -62 -24) centered at (30 -68 -32)
				2	NA	NA	NA	856	(30 -66 -32) to (44 -58 -20) centred at (38 -61 -25)
Ahmed et al., 2019 [26]	33	513	512	1	↓	Yes	No	1056	(26 -78 -40) to (34 -62 -24) centered at (30 -71 -32)
				2	↓	No	No	808	(30 -66 -32) to (44 -58 -20) centered at (38 -61 -25)
Canu et al., 2011 [5]	31	512	568	1	↓	No	No	688	(26 -78 -40) to (34 -68 -24) centered at (30 -73 -29)
Canu et al., 2012 [7]	34	505	528	1	↓	No	No	808	(30 -66 -32) to (44 -58 -20) centered at (38 -61 -25)
Colloby et al., 2014	33	482	496	1	↓	No	No	1088	(26 -78 -40) to (34 -62 -24) centered at (30 -71 -32)

Study Removed	Number of foci	Number of subjects	Min cluster size (mm ³) by ALE algorithm	Cluster number (by size; ordered according to correspondence to main analysis cluster) ^a	Change in cluster size?	Change in peak coordinate by >2 in any direction?	Change in label of peak coordinates?	Extent (mm ³)	Cluster coordinates
[27]				2	↓	No	No	840	(30 -66 -32) to (44 -58 -20) centered at (40 -62 -24)
Farrow et al., 2006 [28]	33	522	552	1	↓	No	No	1056	(26 -78 -40) to (34 -62 -24) centered at (30 -71 -32)
				2	↓	No	No	808	(30 -66 -32) to (44 -58 -20) centered at (38 -61 -25)
Guo et al., 2016 [6]	31	495	544	1	↓	No	No	840	(30 -66 -32) to (44 -58 -20) centred at (38 -61 -25)
Lehmann et al., 2011 [29]	34	499	440	1	↑ (clusters 1 and 2 merged)	Yes	No	2080	(26 -78 -40) to (44 -58 -20) centered at (33 -67 -29)
Mazere et al., 2007 [30]	33	521	504	1	↓	No	No	1056	(26 -78 -40) to (34 -62 -24) centered at (30 -68 -32)
				2	↓	Yes	No	800	(30 -66 -32) to (44 -58 -20) centered at (38 -61 -25)
Möller et al., 2013 [8] ^b	27	409	608	1	↓	Yes	No	624	(24 -78 -30) to (34 -68 -24) centered at (30 -74 -27)
Ossenkoppele et al., 2015 [31]	33	471	424	1	↑ (clusters 1 and 2 merged)	Yes	No	2104	(26 -78 -40) to (44 -58 -20) centered at (33 -67 -29)
Raji et al., 2009 [32]	32	496	440	1	↑ (clusters 1 and 2 merged)	Yes	No	2128	(26 -78 -40) to (44 -58 -20) centered at (33 -67 -29)
Serra et al., 2014 [33]	34	481	432	1	↑ (clusters 1 and 2 merged)	Yes	No	2080	(26 -78 -40) to (44 -58 -20) centered at (33 -67 -29)

Study Removed	Number of foci	Number of subjects	Min cluster size (mm ³) by ALE algorithm	Cluster number (by size; ordered according to correspondence to main analysis cluster) ^a	Change in cluster size?	Change in peak coordinate by >2 in any direction?	Change in label of peak coordinates?	Extent (mm ³)	Cluster coordinates
Toniolo et al., 2018 [9]	32	442	424	1	↑ (clusters 1 and 2 merged)	Yes	No	1512	(26 -78 -40) to (42 -58 -24) centered at (31 -69 -31)

^aIn order of size in mm³ for the full dataset. The order for other studies is in accordance to which clusters are equivalent to the original results from the full analysis.

^bIn the jackknife analysis for Möller et al. (2013), the large AD cluster split into two subclusters (numbered 1 and 2 here) that were no longer contiguous but remained in the same spatial location as the large combined cluster. Another third cluster in left anterior cerebellar regions emerged as significant which had not been found in any of the other analyses.

Table D2. Summary of the effects of jackknifing on each of the clusters from the main ageing and AD analyses.

Cluster from main analysis	Survives thresholding in <i>n</i> one-study removed analyses (%)	Is reduced in size in <i>n</i> one-study removed analyses (%)	Is increased in size in <i>n</i> one-study removed analyses (%)	Is unchanged in size in <i>n</i> one-study removed analyses (%)	Changes peak location by >2 in <i>n</i> one-study removed analyses (%)	Changes peak label in <i>n</i> one-study removed analyses (%)
<i>Healthy ageing</i>						
1	18 (100)	7 (39)	2 (11)	9 (50)	1 (6)	0 (0)
2	18 (100)	6 (33)	9 (50)	3 (17)	1 (6)	0 (0)
3	17 (94)	5 (28)	8 (44)	4 (22)	3 (17)	0 (0)
4	17 (94)	5 (28)	3 (17)	9 (50)	0 (0)	0 (0)
5	15 ^a (83)	4 (22)	1 (6)	10 (56)	1 (6)	0 (0)
<i>Alzheimer's disease</i>						
1	11 ^b (85)	5 (45)	6 ^c (55)	0 (0)	7 (63) ^d	0 (0)
2	11 ^b (85)	5 (45)	6 ^c (55)	0 (0)	6 (55) ^d	0 (0)

^aThis cluster splits into two smaller clusters that are no longer connected in one of the jackknife analyses.

Note that changes in size here refer to any alterations in the cluster size, regardless of whether this change was in one voxel or a large number of voxels.

^bThis includes instances in which cluster 1 and 2 merge, which are counted as survival of each cluster. ^cThis refers to cases in which clusters 1 and 2 merged.

^dThis includes five instances in which clusters 1 and 2 merge.

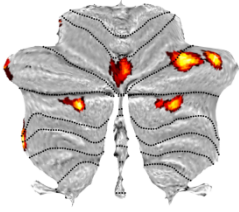
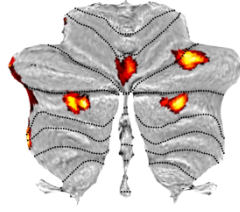
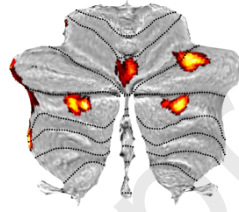
Percentages of changes in cluster properties are based on all instances in which this cluster survives.

a.

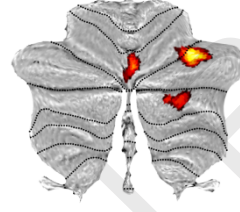
Study removed:

Abe et al., 2008
 $n=73$
 $k=2$ Alexander et al., 2006
 $n=26$
 $k=1$ Antonova et al., 2009
 $n=20$
 $k=5$ Bauer et al., 2012
 $n=36$
 $k=2$ 

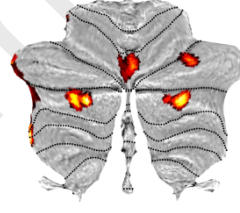
Study removed:

Bauer et al., 2018
 $n=70$
 $k=4$ Bergfield et al., 2010
 $n=29$
 $k=1$ Dickie et al., 2015
 $n=80$
 $k=2$ Draganski et al., 2011
 $n=26$
 $k=2$ 

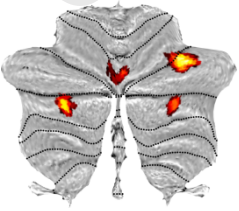
Study removed:

Good et al., 2001
 $n=465$
 $k=1$ Hu et al., 2018
 $n=148$
 $k=5$ Kalpouzos et al., 2009
 $n=45$
 $k=2$ Kalpouzos et al., 2012
 $n=36$
 $k=1$ 

Study removed:

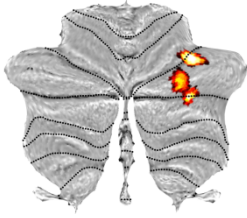
Maguire et al., 2003
 $n=24$
 $k=1$ Salami et al., 2012
 $n=292$
 $k=1$ Steffner et al., 2009
 $n=52$
 $k=1$ Thürling et al., 2014
 $n=34$
 $k=19$ 

Study removed:

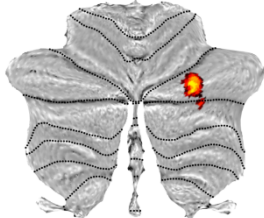
Yu et al., 2017
 $n=438$
 $k=5$ Ziegler et al., 2012
 $n=547$
 $k=1$ 

b.

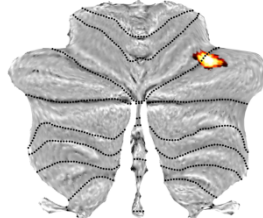
Study removed:
Ahmed et al., 2019
 $n=16$
 $k=2$



Canu et al., 2011
 $n=17$
 $k=4$



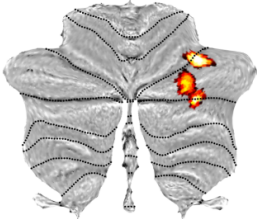
Canu et al., 2012
 $n=24$
 $k=1$



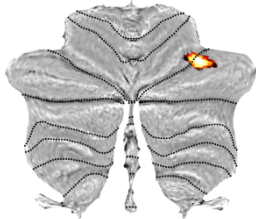
Colloby et al., 2014
 $n=47$
 $k=2$



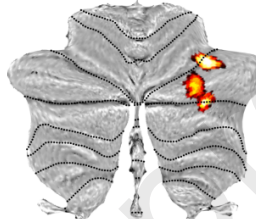
Study removed:
Farrow et al., 2007
 $n=7$
 $k=2$



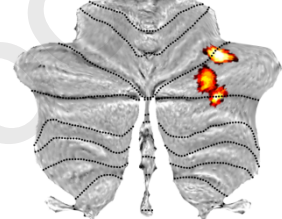
Guo et al., 2016
 $n=34$
 $k=4$



Lehmann et al., 2011
 $n=30$
 $k=1$



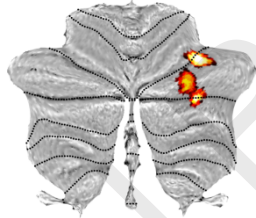
Mazere et al., 2008
 $n=8$
 $k=7$



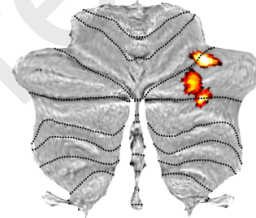
Study removed:
Möller et al., 2013
 $n=120$
 $k=8$



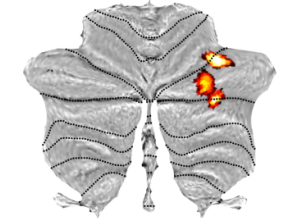
Ossenkoppele et al., 2015
 $n=58$
 $k=2$



Raji et al., 2009
 $n=33$
 $k=3$



Serra et al., 2014
 $n=48$
 $k=1$



Toniolo et al., 2018
 $n=87$
 $k=3$

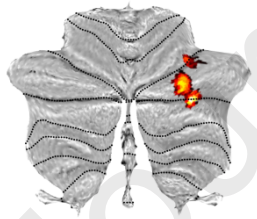
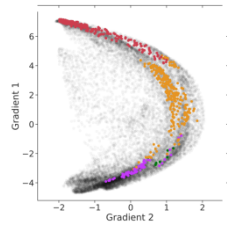


Figure D1. Flatmaps for each of the 18 jackknife analyses for age-related grey matter decline (a) and for the 13 jackknife analyses for atrophy associated with Alzheimer's disease (b). The number of subjects included in each study is indicated by n and the number of coordinates of cerebellar grey matter loss is given by k .

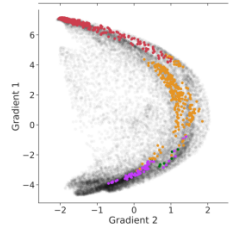
a.

Study removed:

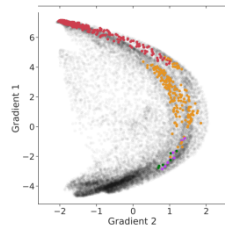
Abe et al., 2008

 $n=73$ $k=2$ 

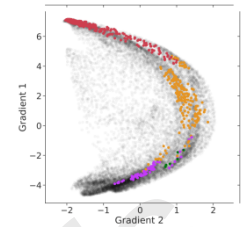
Alexander et al., 2006

 $n=26$ $k=1$ 

Antonova et al., 2009

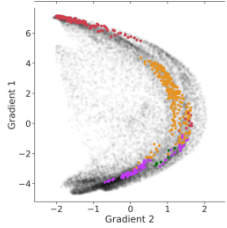
 $n=20$ $k=5$ 

Bauer et al., 2012

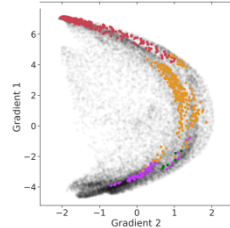
 $n=36$ $k=2$ 

Study removed:

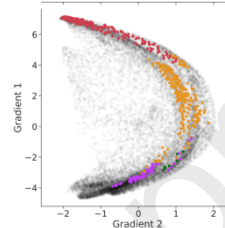
Bauer et al., 2018

 $n=70$ $k=4$ 

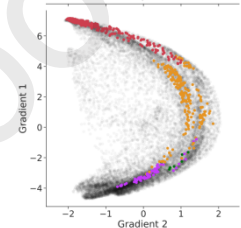
Bergfield et al., 2010

 $n=29$ $k=1$ 

Dickie et al., 2015

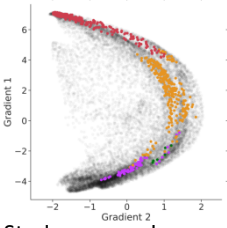
 $n=80$ $k=2$ 

Draganski et al., 2011

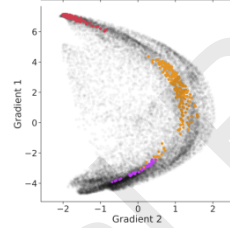
 $n=26$ $k=2$ 

Study removed:

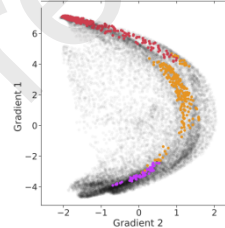
Good et al., 2001

 $n=465$ $k=1$ 

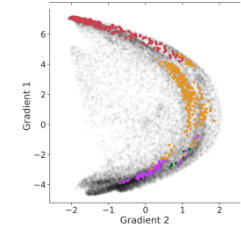
Hu et al., 2018

 $n=148$ $k=5$ 

Kalpouzos et al., 2009

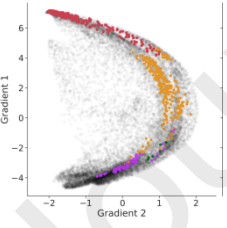
 $n=45$ $k=2$ 

Kalpouzos et al., 2012

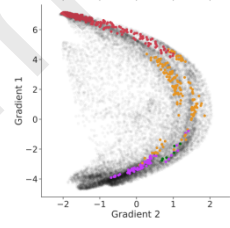
 $n=36$ $k=1$ 

Study removed:

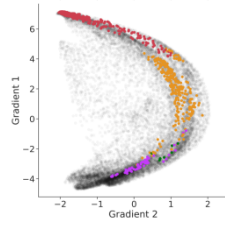
Maguire et al., 2003

 $n=24$ $k=1$ 

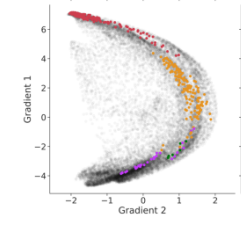
Salami et al., 2012

 $n=292$ $k=1$ 

Steffner et al., 2009

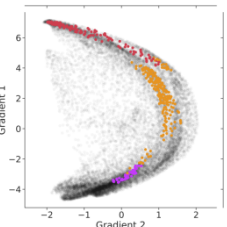
 $n=52$ $k=1$ 

Thürling et al., 2014

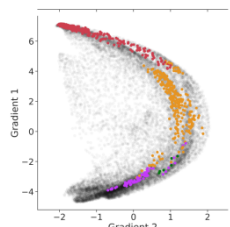
 $n=34$ $k=19$ 

Study removed:

Yu et al., 2017

 $n=438$ $k=5$ 

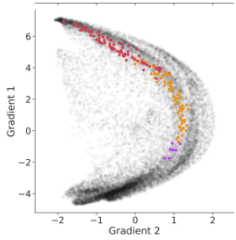
Ziegler et al., 2012

 $n=547$ $k=1$ 

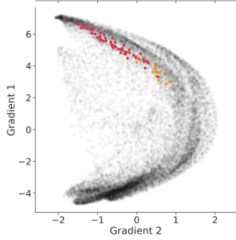
b.

Study removed:

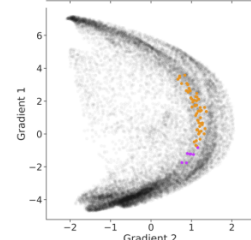
Ahmed et al., 2019

 $n=16$ $k=2$ 

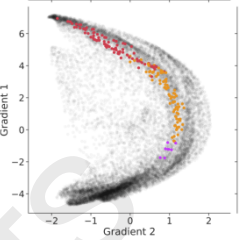
Canu et al., 2011

 $n=17$ $k=4$ 

Canu et al., 2012

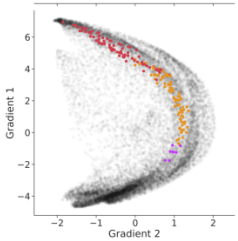
 $n=24$ $k=1$ 

Colloby et al., 2014

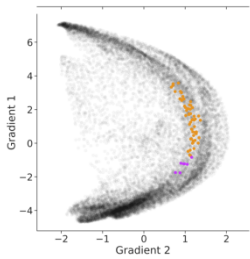
 $n=47$ $k=2$ 

Study removed:

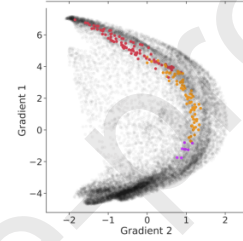
Farrow et al., 2007

 $n=7$ $k=2$ 

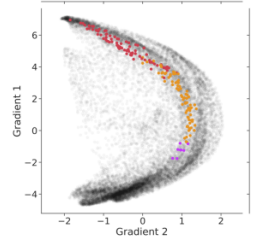
Guo et al., 2016

 $n=34$ $k=4$ 

Lehmann et al., 2011

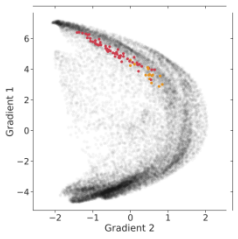
 $n=30$ $k=1$ 

Mazere et al., 2008

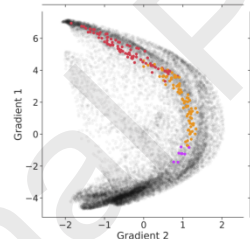
 $n=8$ $k=2$ 

Study removed:

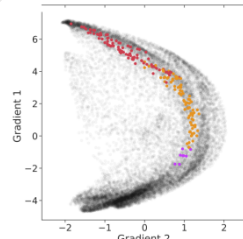
Möller et al., 2013

 $n=120$ $k=8$ 

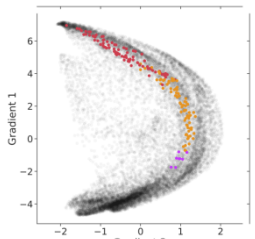
Ossenkuppele et al., 2015

 $n=58$ $k=2$ 

Raji et al., 2009

 $n=33$ $k=3$ 

Serra et al., 2014

 $n=48$ $k=1$ 

Study removed:

Toniolo et al., 2018

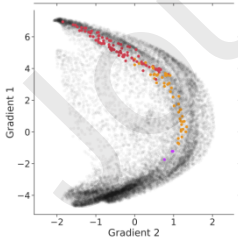
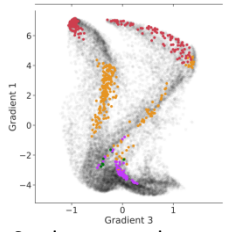
 $n=87$ $k=3$ 

Figure D2. Gradient 1 and 2 values plotted for each of the 18 jackknife analyses of age-related grey matter decline (a) and the 13 analyses for AD (b). The number of subjects included in each study is indicated by n and the number of coordinates of cerebellar grey matter loss is given by k .

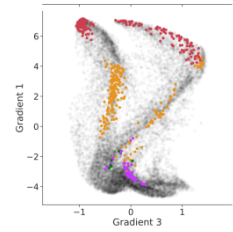
a.

Study removed:

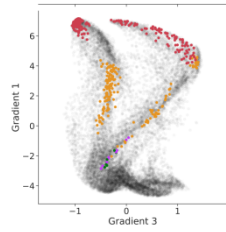
Abe et al., 2008

 $n=73$ $k=2$ 

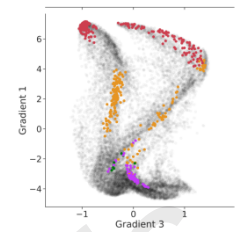
Alexander et al., 2006

 $n=26$ $k=1$ 

Antonova et al., 2009

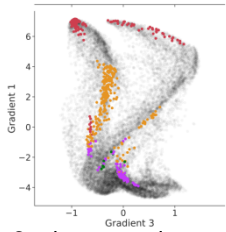
 $n=20$ $k=5$ 

Bauer et al., 2012

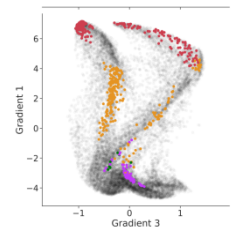
 $n=36$ $k=2$ 

Study removed:

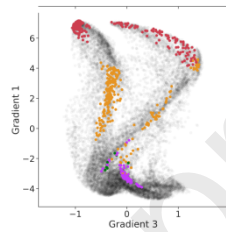
Bauer et al., 2018

 $n=70$ $k=4$ 

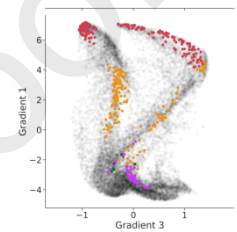
Bergfield et al., 2010

 $n=29$ $k=1$ 

Dickie et al., 2015

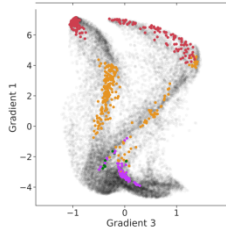
 $n=80$ $k=2$ 

Draganski et al., 2011

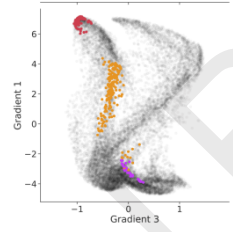
 $n=26$ $k=2$ 

Study removed:

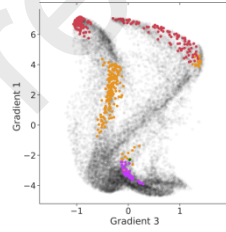
Good et al., 2001

 $n=465$ $k=1$ 

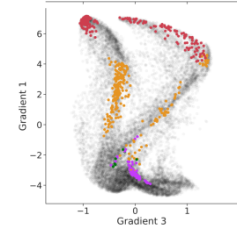
Hu et al., 2018

 $n=148$ $k=5$ 

Kalpouzos et al., 2009

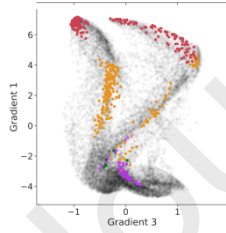
 $n=45$ $k=2$ 

Kalpouzos et al., 2012

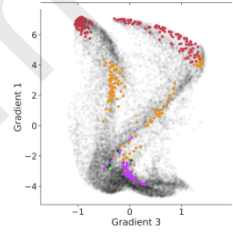
 $n=36$ $k=1$ 

Study removed:

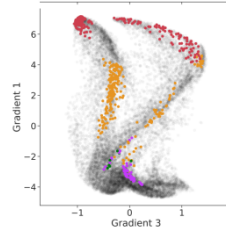
Maguire et al., 2003

 $n=24$ $k=1$ 

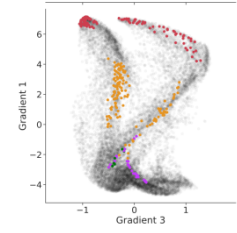
Salami et al., 2012

 $n=292$ $k=1$ 

Steffner et al., 2009

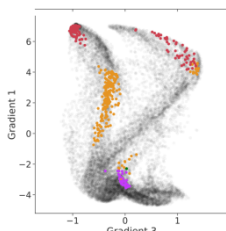
 $n=52$ $k=1$ 

Thürling et al., 2014

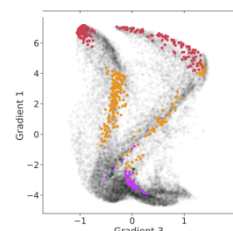
 $n=34$ $k=19$ 

Study removed:

Yu et al., 2017

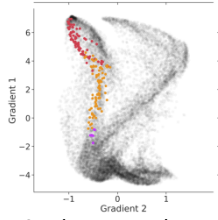
 $n=438$ $k=5$ 

Ziegler et al., 2012

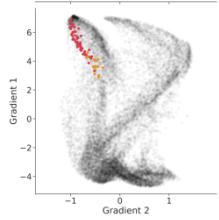
 $n=547$ $k=1$ 

b.

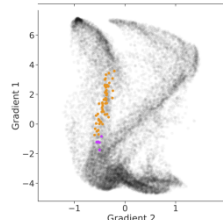
Study removed:
Ahmed et al., 2019
 $n=16$
 $k=2$



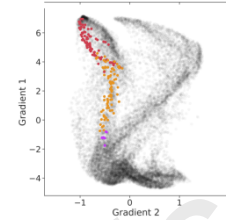
Canu et al., 2011
 $n=17$
 $k=4$



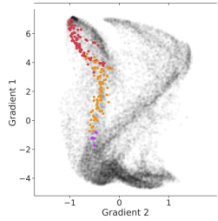
Canu et al., 2012
 $n=24$
 $k=1$



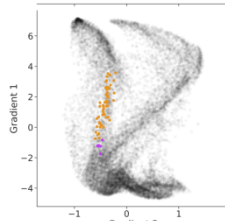
Colloby et al., 2014
 $n=47$
 $k=2$



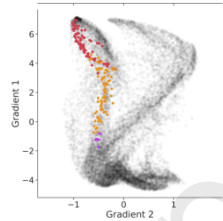
Study removed:
Farrow et al., 2007
 $n=7$
 $k=2$



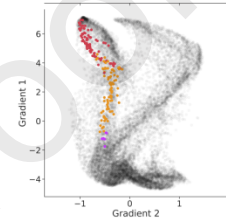
Guo et al., 2016
 $n=34$
 $k=4$



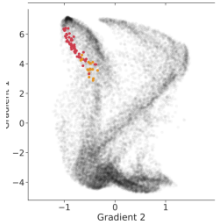
Lehmann et al., 2011
 $n=30$
 $k=1$



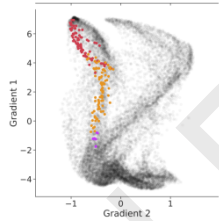
Mazere et al., 2008
 $n=8$
 $k=2$



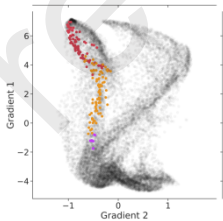
Study removed:
Möller et al., 2013
 $n=120$
 $k=8$



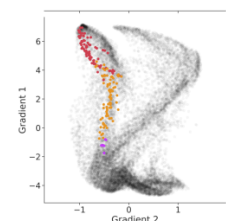
Ossenkoppele et al., 2015
 $n=58$
 $k=2$



Raji et al., 2009
 $n=33$
 $k=3$



Serra et al., 2014
 $n=48$
 $k=1$



Study removed:
Toniolo et al., 2018
 $n=87$
 $k=3$

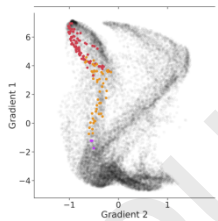


Figure D3. Gradient 1 and 3 values plotted for each of the 18 jackknife analyses of age-related grey matter decline (a) and the 13 jackknife analyses for AD (b). The number of subjects included in each study is indicated by n and the number of coordinates of cerebellar grey matter loss is given by k .

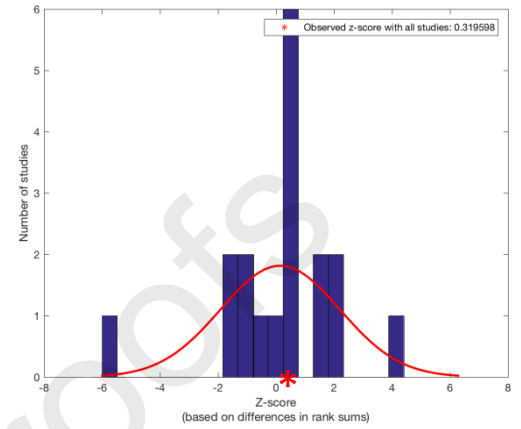
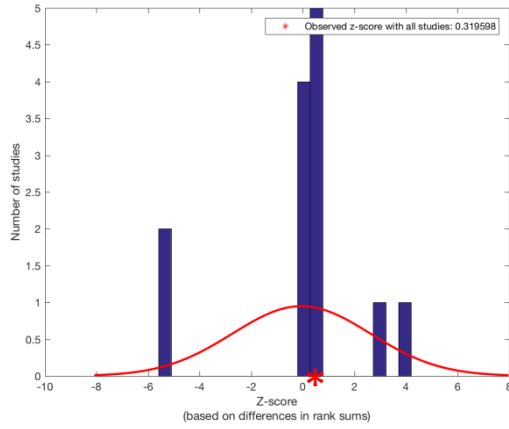
13 Alzheimer's disease jackknife tests

18 healthy ageing

jackknife tests

a.

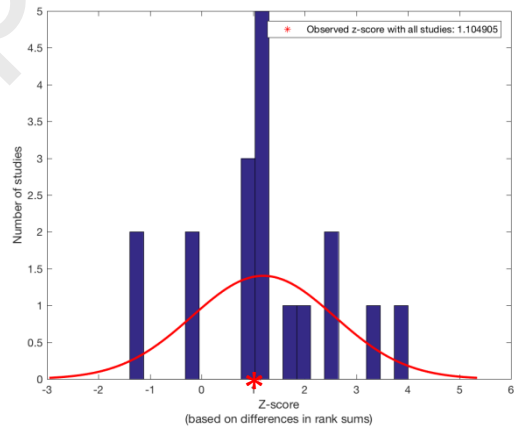
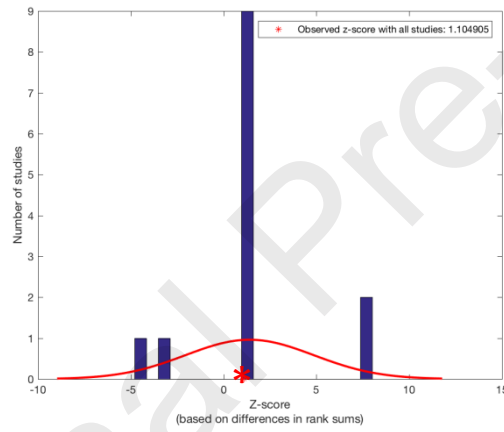
Observed z-score across all studies: .320



b.

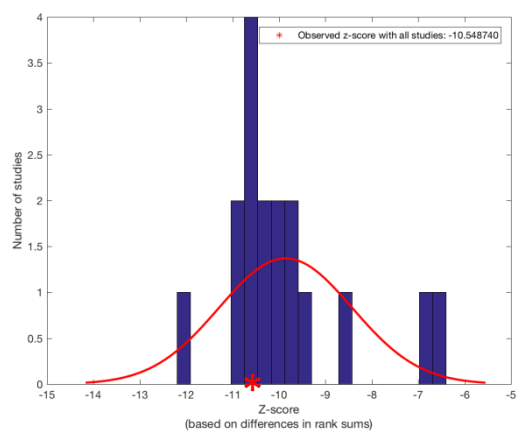
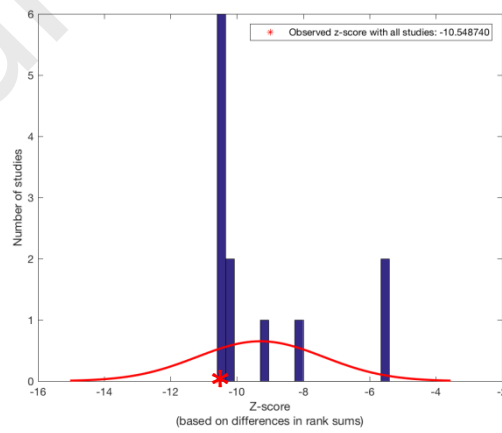
Observed z-score across all studies: 1.105

Number of studies



c.

Observed z-score across all studies: -10.549



Z-score (based on differences in rank sums)

Figure D4. Summary of differences in gradient values between AD and healthy ageing following a jackknife procedure.

Panels a, b, and c represent jackknife analyses for gradients 1, 2, and 3, respectively. The differences between gradient values for AD and ageing were calculated as z-scores based on the Wilcoxon rank sum test. Left panels show results of comparing the gradient values from the total healthy ageing sample (18 studies) to the gradient values from the Alzheimer's disease data set with a given study removed from the analysis (i.e. 12 studies rather than the full 13). Right panels show results of comparing the gradient values from the total AD sample (13 studies) to the gradient values from the healthy ageing data set with a given study removed from the analysis (i.e. 17 studies rather than the full 18). The red asterisk marks the observed mean difference between all AD and all healthy ageing studies.

References

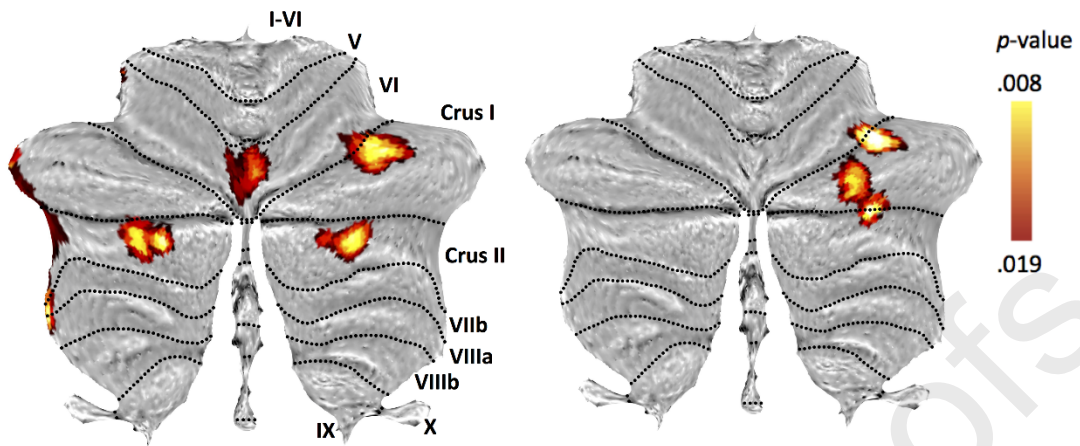
- [1] Hu S, Ide JS, Chao HH, Castagna B, Fischer KA, Zhang S, et al. Structural and functional cerebral bases of diminished inhibitory control during healthy aging. *Hum Brain Mapp* 2018;39:5085–5096. doi:10.1002/hbm.24347.
- [2] Antonova E, Parslow D, Brammer M, Dawson GR, Jackson SHDD, Morris RG. Age-related neural activity during allocentric spatial memory. *Memory* 2009;17:125–43. doi:10.1080/09658210802077348.
- [3] Yu T, Korgaonkar MS, Grieve SM. Gray matter atrophy in the cerebellum—Evidence of increased vulnerability of the crus and vermis with advancing age. *The Cerebellum* 2017;16:388–97. doi:10.1007/s12311-016-0813-x.
- [4] Kalpouzos G, Chételat G, Landeau B, Clochon P, Viader F, Eustache F, et al. Structural and metabolic correlates of episodic memory in relation to the depth of encoding in normal aging. *J Cogn Neurosci* 2009;21:372–89. doi:10.1162/jocn.2008.21027.
- [5] Canu E, McLaren DG, Fitzgerald ME, Bendlin BB, Zoccatelli G, Alessandrini F, et al. Mapping the structural brain changes in Alzheimer's disease: The independent contribution of two imaging modalities. *Adv Alzheimer's Dis* 2011;2:487–98. doi:10.3233/978-1-60750-793-2-487.
- [6] Guo CC, Tan R, Hodges JR, Hu X, Sami S, Hornberger M. Network-selective vulnerability of the human cerebellum to Alzheimer's disease and frontotemporal dementia. *Brain* 2016;139:1527–38. doi:10.1093/brain/aww003.
- [7] Canu E, Frisoni GB, Agosta F, Pievani M, Bonetti M, Filippi M. Early and late onset Alzheimer's disease patients have distinct patterns of white matter damage. *Neurobiol Aging* 2012;33:1023–33. doi:10.1016/j.neurobiolaging.2010.09.021.
- [8] Möller C, Vrenken H, Jiskoot L, Versteeg A, Barkhof F, Scheltens P, et al. Different patterns of gray matter atrophy in early- and late-onset Alzheimer's disease. *Neurobiol Aging* 2013;34:2014–22. doi:http://dx.doi.org/10.1016/j.neurobiolaging.2013.02.013.
- [9] Toniolo S, Serra L, Olivito G, Marra C, Bozzali M, Cercignani M. Patterns of cerebellar gray matter atrophy across Alzheimer's disease progression. *Front Cell Neurosci* 2018;12:1–8. doi:10.3389/fncel.2018.00430.
- [10] Jacobs HIL, Hopkins DA, Mayrhofer HC, Bruner E, Van Leeuwen FW, Raaijmakers W, et al. The cerebellum in Alzheimer's disease: Evaluating its role in cognitive decline. *Brain* 2018;141:37–47. doi:10.1093/brain/awx194.
- [11] Abe O, Yamasue H, Aoki S, Suga M, Yamada H, Kasai K, et al. Aging in the CNS: comparison of gray/white matter volume and diffusion tensor data. *Neurobiol Aging* 2008;29:102–16. doi:10.1016/j.neurobiolaging.2006.09.003.
- [12] Alexander GE, Chen K, Merkley TL, Reiman EM, Caselli RJ, Aschenbrenner

- M, et al. Regional network of magnetic resonance imaging gray matter volume in healthy aging. *Neuroreport* 2006;17:951–6. doi:10.1097/01.wnr.0000220135.16844.b6.
- [13] Bauer E, Gebhardt H, Gruppe H, Gallhofer B, Sammer G. Altered negative priming in older subjects: First evidence from behavioral and neural level. *Front Hum Neurosci* 2012;6:1–10. doi:10.3389/fnhum.2012.00270.
- [14] Bauer E, Sammer G, Toepper M. Performance level and cortical atrophy modulate the neural response to increasing working memory load in younger and older adults. *Front Aging Neurosci* 2018;10:1–15. doi:10.3389/fnagi.2018.00265.
- [15] Bergfield KL, Hanson KD, Chen K, Teipel SJ, Hampel H, Rapoport SI, et al. Age-related networks of regional covariance in MRI gray matter: Reproducible multivariate patterns in healthy aging. *Neuroimage* 2010;49:1750–9. doi:10.1016/j.neuroimage.2009.09.051.
- [16] Dickie DA, Job DE, Gonzalez DR, Shenkin SD, Wardlaw JM. Use of brain MRI atlases to determine boundaries of age-related pathology: the importance of statistical method. *PLoS One* 2015;10:e0127939. doi:10.1371/journal.pone.0127939.
- [17] Draganski B, Ashburner J, Hutton C, Kherif F, Frackowiak RSJJ, Helms G, et al. Regional specificity of MRI contrast parameter changes in normal ageing revealed by voxel-based quantification (VBQ). *Neuroimage* 2011;55:1423–34. doi:10.1016/j.neuroimage.2011.01.052.
- [18] Good CD, Johnsrude IS, Ashburner J, Henson RNA, Friston KJ, Frackowiak RSJ. A voxel-based morphometric study of ageing in 465 normal adult human brains. *Neuroimage* 2001;14:21–36. doi:10.1006/nimg.2001.0786.
- [19] Kalpouzos G, Chételat G, Baron JC, Landeau B, Mevel K, Godeau C, et al. Voxel-based mapping of brain gray matter volume and glucose metabolism profiles in normal aging. *Neurobiol Aging* 2009;30:112–24. doi:10.1016/j.neurobiolaging.2007.05.019.
- [20] Kalpouzos G, Persson J, Nyberg L. Local brain atrophy accounts for functional activity differences in normal aging. *Neurobiol Aging* 2012;33:e1–13. doi:10.1016/j.neurobiolaging.2011.02.021.
- [21] Maguire EA, Frith CD. Aging affects the engagement of the hippocampus during autobiographical memory retrieval. *Brain* 2003;126:1511–23. doi:10.1093/brain/awg157.
- [22] Salami A, Eriksson J, Nyberg L. Opposing effects of aging on large-scale Brain systems for memory encoding and cognitive control. *J Neurosci* 2012;32:10749–57. doi:10.1523/JNEUROSCI.0278-12.2012.
- [23] Steffener J, Brickman AM, Rakitin BC, Gazes Y, Stern Y. The impact of age-related changes on working memory functional activity. *Brain Imaging Behav* 2009;3:142–53. doi:10.1007/s11682-008-9056-x.
- [24] Thürling M, Galuba J, Thieme A, Burciu RG, Goricke S, Beck A, et al. Age effects in storage and extinction of a naturally acquired conditioned eyeblink response. *Neurobiol Learn Mem* 2014;109:104–12. doi:10.1016/j.nlm.2013.12.007.
- [25] Ziegler G, Dahnke R, Jäncke L, Yotter RA, May A, Gaser C. Brain structural trajectories over the adult lifespan. *Hum Brain Mapp* 2012;33:2377–89. doi:10.1002/hbm.21374.
- [26] Ahmed RM, Landin-Romero R, Liang CT, Keogh JM, Henning E, Strikwerda-Brown C, et al. Neural networks associated with body composition in

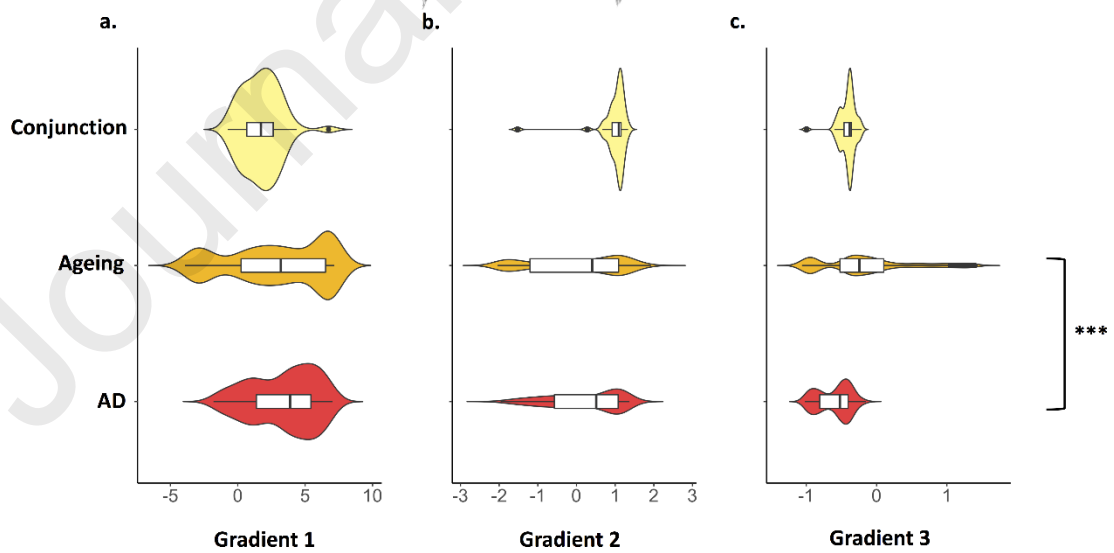
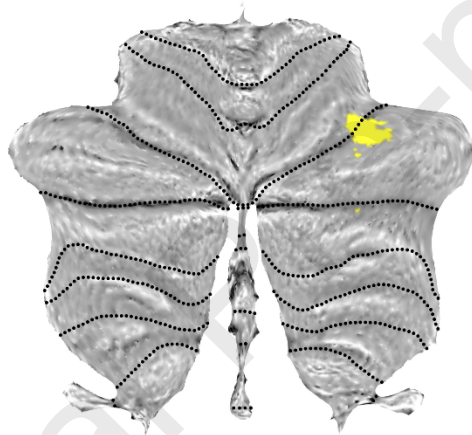
- frontotemporal dementia. *Ann Clin Transl Neurol* 2019;6:1707–17. doi:10.1002/acn3.50869.
- [27] Colloby SJ, O'Brien JT, Taylor JP. Patterns of cerebellar volume loss in dementia with Lewy bodies and Alzheimer's disease: A VBM-DARTEL study. *Psychiatry Res - Neuroimaging* 2014;223:187–91. doi:10.1016/j.pscychresns.2014.06.006.
- [28] Farrow TFD, Thiyagesh SN, Wilkinson ID, Parks RW, Ingram L, Woodruff PWR. Fronto-temporal-lobe atrophy in early-stage Alzheimer's disease identified using an improved detection methodology. *Psychiatry Res* 2007;155:11–9. doi:10.1016/j.pscychresns.2006.12.013.
- [29] Lehmann M, Crutch SJ, Ridgway GR, Ridha BH, Barnes J, Warrington EK, et al. Cortical thickness and voxel-based morphometry in posterior cortical atrophy and typical Alzheimer's disease. *Neurobiol Aging* 2011;32:1466–76. doi:10.1016/j.neurobiolaging.2009.08.017.
- [30] Mazère J, Prunier C, Barret O, Guyot M, Hommet C, Guilloteau D, et al. In vivo SPECT imaging of vesicular acetylcholine transporter using [123I]-IBVM in early Alzheimer's disease. *Neuroimage* 2008;40:280–8. doi:10.1016/j.neuroimage.2007.11.028.
- [31] Ossenkoppele R, Pijnenburg YAL, Perry DC, Cohn-Sheehy BI, Scheltens NME, Vogel JW, et al. The behavioural/dysexecutive variant of Alzheimer's disease: Clinical, neuroimaging and pathological features. *Brain* 2015;138:2732–49. doi:10.1093/brain/awv191.
- [32] C.A. R, O.L. L, L.H. K, O.T. C, J.T. B, Raji CA, et al. Age, Alzheimer disease, and brain structure. *Neurology* 2009;73:1899–905. doi:10.1212/WNL.0b013e3181c3f293.
- [33] Serra L, Fadda L, Perri R, Spanò B, Marra C, Castelli D, et al. Constructional apraxia as a distinctive cognitive and structural brain feature of pre-senile Alzheimer's disease. *J Alzheimer's Dis* 2014;38:391–402. doi:10.3233/JAD-130656.

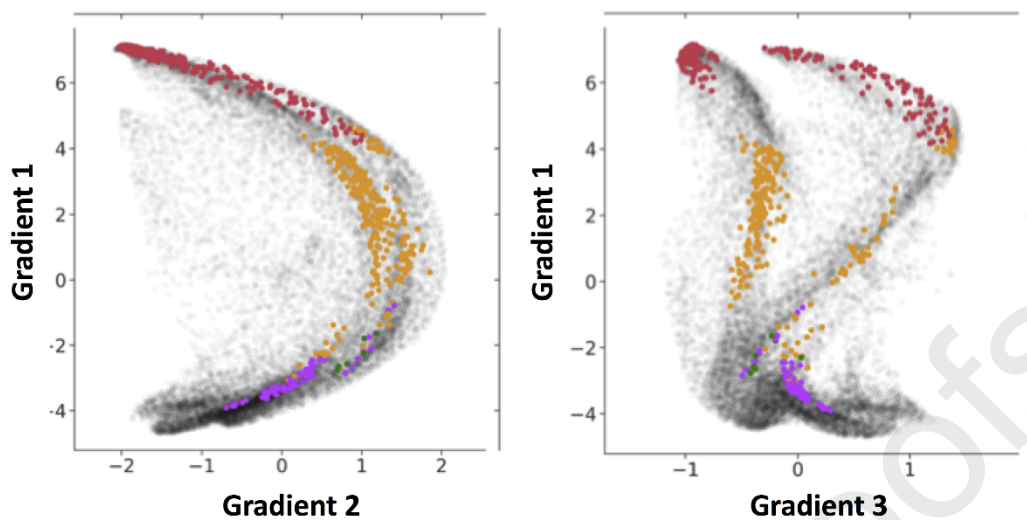
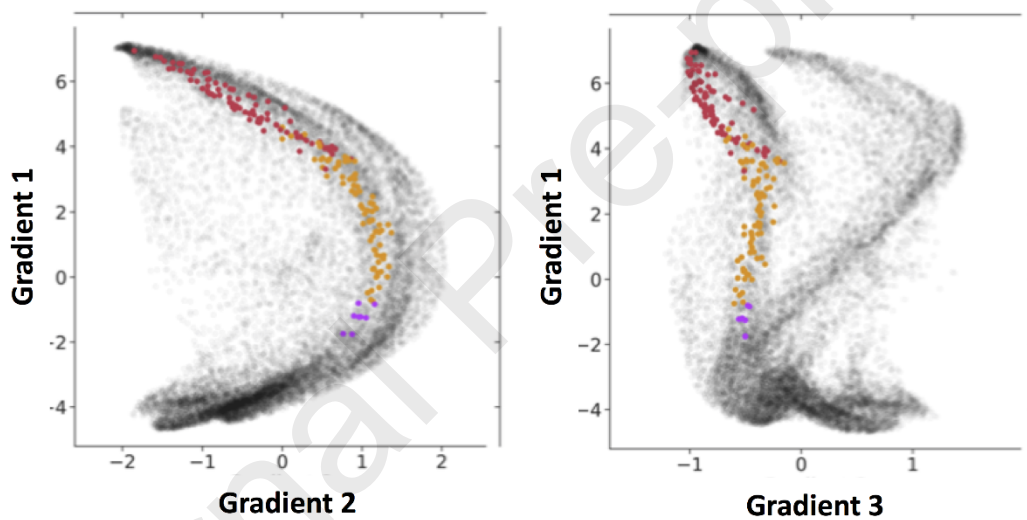
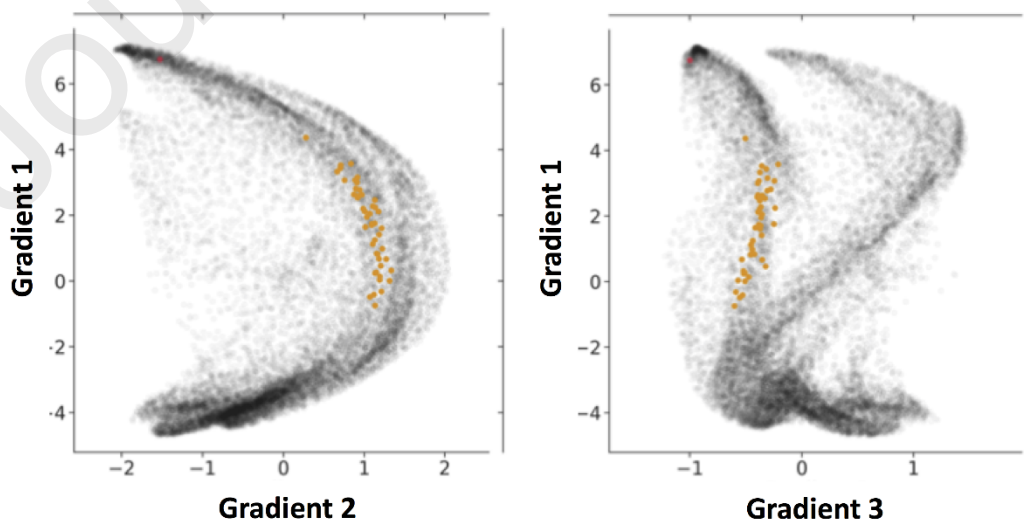
a. Younger > older adults

b. Controls > Alzheimer's disease

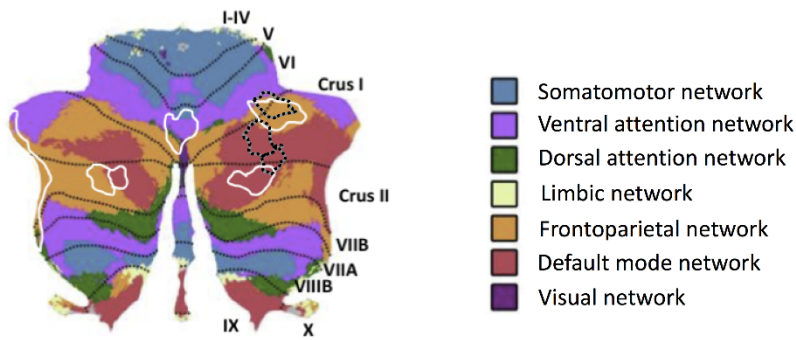


c. Conjunction age and AD



a. Healthy ageing**b. Alzheimer's disease****c. Conjunction of ageing and Alzheimer's disease**

d. Intrinsic connectivity networks based on Buckner et al., 2011



e. Functional mapping based on King et al., 2019

1 Motor planning, left-hand presses, interference resolution

3 Visual working memory, saccades, visual letter recognition

5 Active maintenance, divided attention, mental arithmetic

7 Emotion processing, narrative, language processing

10 Visual letter recognition, autobiographical recall, interference resolution

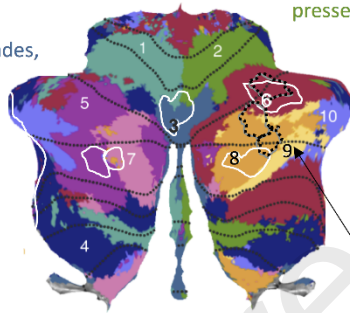
2 Motor planning, right-hand presses, divided attention

4 Divided attention, action observation, motor planning

6 Active maintenance, divided attention, verbal fluency

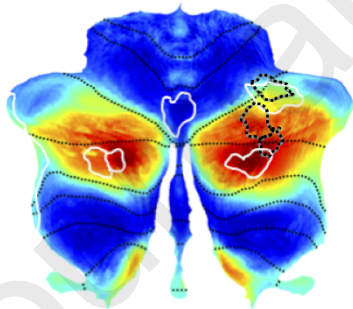
8 Language processing, word comprehension, narrative

9 Word comprehension, verbal fluency, mental arithmetic

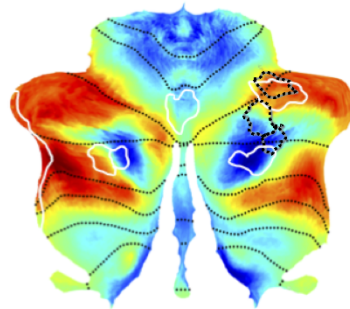


f. Continuous mappings of functional gradients based on Guell et al., 2018

Gradient 1: motor vs. cognitive processing



Gradient 2: degree of task focus



Gradient 3: hemispheric differences in cognitive processing

